DocuServe

Electronic Delivery Cover Sheet

Caltech Library Services

Star Formation in the Local Universe – EES2010
C. Charbonnel and T. Montmerle (eds)
EAS Publications Series, **51** *(2011) 245-287*

PRE–MAIN SEQUENCE EVOLUTION OF STAR FORMING REGIONS AND YOUNG CLUSTERS

F. Palla[1]

Abstract. This review covers a variety of topics related to the properties of Pre–Main Sequence stars in star forming regions, young clusters and associations. Some recent developments of theoretical models of PMS evolution are discussed, with emphasis on the role of magnetic fields in low-mass stars and their impact on observable quantities. Critical tests on the comparison between model predictions and observations are presented for stars across the mass spectrum. The issue of the formation and early evolution of massive stars is addressed, with emphasis on clustered versus isolated objects. After a brief historical background on the derivation of the Initial Mass Function, current representations of this quantity are discussed. The issue of the duration of the star formation process is dealt with using the results of age dating methods for young stars, mainly based on the property of Lithium depletion during PMS evolution. A recent analysis of the properties of the stellar population of the Orion Nebula Cluster is presented with the resulting IMF and age distributions. Finally, a discussion of recent determinations of the metallicity distribution of young stars in clusters and associations closes the review.

1 Introduction

This series of lectures deals with a variety of topics related to the properties of the early evolution of stars in clusters and associations. These include a brief overview of recent developments in the theoretical models of Pre–Main Sequence (hereafter, PMS) evolution, followed by a discussion of critical observational tests for such models provided by the study of stars over the entire mass spectrum, from very low-mass stars and brown dwarfs to massive objects. By its nature, PMS evolution follows, and is entirely dependent on the star formation process, a subject that has been covered by other authors during the school (in particular, see the contributions by R. Klessen & A.J. Maury). Nevertheless, I will address

[1] INAF-Osservatorio Astrofisico di Arcetri, L.go E. Fermi, 5, 50125 Firenze, Italy

DOI: 10.1051/eas/1151013

topics that are naturally linked to star formation, such as the properties of massive stars in clusters and in isolation, the initial mass function (IMF), and the question of stellar ages that directly bears on the problem of the duration of star formation.

The lectures included a presentation of the basic theoretical results of PMS evolution established by the early work of Hayashi, Salpeter, Iben and of the impact that modern protostellar evolution has had on these classical studies. As these issues have been described in the contribution to the Proceedings of the X-th Aussois School of PNPS/INSU/CNRS on *Star Formation and The Physics of Young Stars* that took place in 2000 (EAS Publications Series, Volume 3, eds. J. Bouvier & J.-P. Zahn, EDP Sciences, 2002), they will not be repeated here and the interested reader can refer to that publication for a full account.

Since the main theme of these lectures concerns the properties of young stars, it was appropriate to start the presentation paying hommage to the work of Evry Schatzman, to whom the Ecole de Physique Stellaire is now dedicated. Of particular interest is the autobiographical review that Schatzman wrote in 1996 (ARA&A, Vol. 34) in which two aspects stand out from his narration: the origin of his passion for doing research (*... passion and pleasure for exploring unknown countries of knowledge...*), and the need to transmit a message (*... I always tried to transmit a message...*). These two characteristics have marked his scientific research that developed under very hard circumstances for a young Jewish with an interest in astrophysics during the 1940s. In this respect, Schatzman's reflections are similar to those expressed by another contemporary and prominent figure of stellar astrophysics, E.E. Salpeter (see his 2002 ARA&A review), whose work will also be mentioned in these lectures in the context of the IMF.

2 Pre–main sequence evolution: Available theoretical models

Unlike the previous highly dynamical protostellar phase, the PMS evolution of a star can be followed by models in hydrostatic and thermal equilibrium. These models are much easier to construct and less subject to numerical inaccuracies. Various groups have developed models of varying complexity with special attention to the implementation of input physics (equation of state, opacity, treatment of convection, etc.) using the best available prescriptions. The location of optically visible PMS stars in the HR diagram combined with the use of theoretical evolutionary tracks and isochrones has allowed researchers to derive fundamental quantities of stellar clusters and associations, such as the distribution of stellar masses and ages to contruct the IMF and the star formation history, respectively. Most of the currently used models have been developed in the late 1990s/beginning of 2000 and include Baraffe *et al.* (1998), D'Antona & Mazzitelli (1997), Palla & Stahler (1999; hereafter PS99), and Siess *et al.* (2000). Other available models are those of the Yale group (YREC, Demarque *et al.* 2008), the Pisa group (FRANEC, Degl'Innocenti *et al.* 2008), the Paris group (CESAM, Lebreton & Michel 2008), the Dartmouth group (DSEP08; Dotter *et al.* 2008). Thus, there is ample choice for comparison with observational data. However, since the models are computed using different prescriptions for the input physics, discrepancies are present among

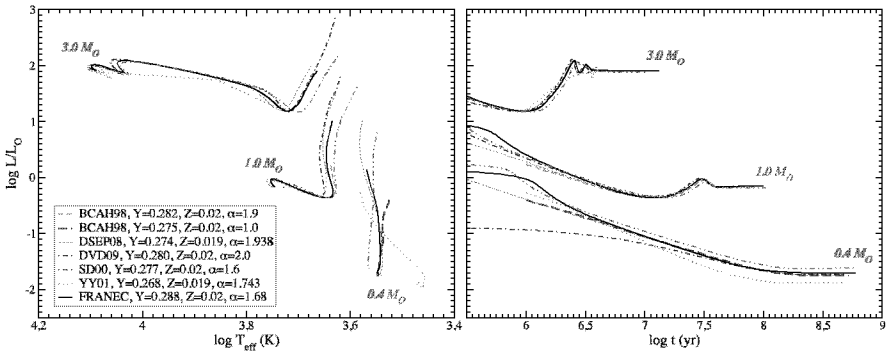

Fig. 1. Comparison of the predictions of different PMS evolutionary models, computed for a solar abundance. The left panel shows the tracks in the (L, $T_{\rm eff}$)–plane, while the right panel is for (L, age). (From Tognelli *et al.* 2011).

the theoretical predictions. One of the most significant difference comes from the adopted boundary conditions. These vary from a simplified $T(\tau)$ relation to specify the surface conditions to realistic atmospheric models which are particularly important for low-mass stars (see the discussion in Baraffe *et al.* 1998). Another important ingredient is the treatment of convection which is usually accounted for using the mixing length approximation, apart from the FRANEC code that adopts the Canuto-Mazzitelli treatment of turbulent convection. A comparison of the predictions of various models is shown in Figure 1.

Several models also include the effects of rotation and magnetic fields, although still in an approximate way. D'Antona *et al.* (2000) presented a first analysis of the effects of surface magnetic fields on the PMS evolution of solar-type stars, with particular emphasis on its effect on the stellar radius and the amount of lithium depletion. Assuming that the magnetic field B is generated by rotation and that its thermal effect is valid for $B^2 \ll P$, where P is the pressure, the phenomenological effect of the magnetic field is expressed through a modification of the Schwarzschild criterion for convection instability of the form $\nabla_{\rm rad} > \nabla_{\rm ad} + \delta$, where $\delta = B^2/(B^2 + \gamma P)$ and γ is the ratio of the specific heats. Indeed, in the interiors of very low-mass stars and BDs the magnetic pressure ($\lesssim 10^7$ dyn cm^{-2}) is orders of magnitude lower than the gas pressure ($10^{12} - 10^{16}$ dyn cm^{-2}; *e.g.*, Chabrier & Baraffe 2000). Thus, for small values of δ, the convective gradient is close to the unperturbed gradient plus δ. This prescription follows the Gough–Tayler (1966) criterion for convective instability. The magnetic inhibition parameter δ is a local variable whose value changes as function of the radial position inside the star. The usual assumption is to take $\delta(R) =$ constant (see also Mullan & Macdonald 2001).

The resulting evolution turns out to be quite sensitive to the values of the surface magnetic field, yielding cooler models and lower lithium depletions than in the case of no magnetic field. Similar results have been obtained more recently by Macdonald & Mullan (2010) who constructed evolutionary sequences of low-mass

stars including the effects of the inhibition of convection due to the presence of a magnetic field. However, Chabrier *et al.* (2007) have criticized such approach arguing that the strength of the magnetic field required to inhibit convection in a core of a low-mass star would be implausibly high and likely unstable. As an alternative, they have simulated the global effects of the magnetic field by reducing the value of the mixing length parameter, $\alpha = l/H_p$ from a canonical value of 1.5–1.9, necessary to fit the Sun, to the smaller value of $\alpha < 1$. However, in order to obtain the same quantitative effect on the effective temperature and radii, Chabrier *et al.* needed to introduce a second parameter related to the presence of large spots on the stellar surface. We will return in Section 6 to the effects of the magnetic field on models of lithium depletion.

3 Observational tests of PMS stars

Since PMS evolution begins when the preceding main accretion phase is over (*i.e.*, when the accretion time scale becomes longer compared to the Kelvin-Helmoltz contraction time), it is important to briefly discuss the main results of protostar evolution as it determines the initial condition for PMS contraction. A key property is the existence of a mass–radius relation for accreting protostellar cores. This relation finds its physical origin in the thermostatic nature of deuterium burning once the protostar reaches the critical ignition temperature ($\sim 10^6$ K). As a result of deuterium burning, first at the center and then in a subsurface shell, protostars never attain large radii. The radius remains typically 3–5 times larger than the corresponding value on the ZAMS, but a factor of ten, or more, smaller than the large values predicted by the classical theory of PMS evolution (Iben, Hayashi, Cameron, etc.) that ignored the impact of protostellar evolution. Another important feature of protostars is that their internal structure departs significantly from the assumption of thermal convection. In the standard PMS theory, all stars are assumed to be fully convective objects as a result of the large initial radii. However, in low-mass protostars convection is due to central deuterium burning, while protostars more massive than about $2\,M_\odot$ are radiatively stable in the inner regions, and possess a thick convective mantle maintained by deuterium burning. Thus, these stars are thermally unrelaxed at the beginning of the PMS evolution and must undergo non-homologous quasi-static contraction.

These two properties have a profound impact on the calculation of PMS evolutionary models and the resulting HR diagram. First, compared to the classical set of PMS tracks, the new tracks occupy a much more limited portion of the diagram. The reason is that the older tracks correspond to stellar radii too large to be attained during protostellar accretion. Thus, the starting luminosities (proportional to R_*^2) are much lower than previously envisioned. In addition, the surface temperature of these stars begin higher. Notice also that the birthline intersects the main sequence at a mass $M_* \sim 8\,M_\odot$: this point represents the critical stellar configuration in which hydrogen burning has stopped gravitational contraction while the star is still growing in mass. More massive stars, therefore, have no PMS phase at all, but appear directly on the main sequence once they are optically

revealed. The exact mass at which the birthline merges into the ZAMS depends on the accretion history and increases as the mass accretion rate increases (for an extended discussion, see the contribution by A. Maeder in this book).

In the following, I will review some important empirical tests on young stars of different mass that have been carried out in the recent past that allow the reader to better appreciate limitations and merits of the theoretical background described so far. For practical purposes, considering the vast literature on the topic, I will select the relevant information obtained in two main fields: the study of eclipsing binary systems for the determination of accurate stellar parameters, and the constraints on the initial conditions for the youngest stars in each mass interval. As usual, I will cover separately low-mass ($M_* \lesssim 2\,M_\odot$), intermediate-mass ($2 \lesssim M/M_\odot \lesssim 8$), and massive ($M \gtrsim 8\,M_\odot$) stars.

3.1 Low-mass stars and brown dwarfs

The study of eclipsing binary systems provides one of the most precise ($\lesssim$2%) and accurate methods for the measurement of fundamental stellar parameters (mass, radius, luminosity, gravity, effective temperature, and distance). They also serve as a critical test of theoretical mass derived from evolutionary models. To date, about thirty dynamical mass measurements of both eclipsing and non-eclipsing binary systems have been obtained, most for stars with mass $\gtrsim 0.5\,M_\odot$, reaching a precision better than 10% (*e.g.*; Mathieu *et al.* 2007). On average, models predict masses to within 20%, but predictions on individual stars have up to 50% uncertainty. The primary limitations are systematic errors in stellar properties (effective temperature, luminosity, radii). However, in a few cases masses and radii have been measured with very high accuracy, thus allowing a rigourous test of the predictions of theoretical models. This is the case of the eclipsing binary system CM Dra composed by two dM4.5 ($\sim 0.2\,M_\odot$) main sequence stars (age $\sim$4 Gyr), whose components mass and radius have been measured with relative uncertainty below 1% (Morales *et al.* 2009).

As of 2007, all the studied systems had mass $M \gtrsim 0.5\,M_\odot$. Hence, the need to extend the analysis to lower mass systems, in a domain where the uncertainties in the stellar models are still the largest due to the poorly known (and admittedly complicated) physics needed to treat the effects of convection, magnetic fields and stellar opacities at low temperatures. Since then, the situation has improved with the discovery of several systems, including two twin brown dwarfs. The current census of the known PMS eclipsing binaries includes ASAS J052821 + 0338.5 in the Ori Ia association ($M_{p,s} = 1.38, 1.33\,M_\odot$; Stempels *et al.* 2008); RXJ 0529.4 + 0041A also in Ori Ia ($M_{p,s} = 1.27, 0.93\,M_\odot$; Covino *et al.* 2004); V1174 Ori in Ori Ic ($M_{p,s} = 1.0, 0.7\,M_\odot$; Stassun *et al.* 2004); Par 1802 in Ori Id (the Orion Nebula Cluster, ONC; $M_{p,s} = 0.41, 0.41\,M_\odot$; Cargile *et al.* 2008); JW 380 ($M_{p,s} = 0.26, 0.15\,M_\odot$; Irwin *et al.* 2007) in Ori Id; and 2MASS J05352184–0546085 also in Ori Id ($M_{p,s} = 0.05, 0.03\,M_\odot$; Stassun *et al.* 2006). Remarkably, all these systems belong to the Orion complex, a fact that could be used to infer reliable stellar ages as an independent clock for the time history of the associations.

Among the lowest mass members, the Par 1802 system stands out as a system with two identical stars with mass ratio $q = 0.98 \pm 0.01$ in a nearly circular orbit with period of 4.7 day. The large radii of both components ($\sim$1.75 $R_\odot$) testify of their youth ($\sim$1 Myr). Owing to the same mass, the stars are expected to have the same values of temperatures, radii and luminosities. However, further observations by Stassun *et al.* (2008) have shown surprising differences in these quantities with temperatures varying by $\sim$300 K (about 10%), radii by 5%, and luminosities by a factor of $\sim$2. Such variations have been interpreted as due to a difference in the epoch of formation of the two components (by about a few 10^5 yr), or by different surface magnetic field properties that are expected to alter the radii and temperatures (but not the luminosity).

A similar reversal in the temperatures of the primary and secondary was also observed in the brown dwarf eclipsing binary 2MASS J0535, contrary to the expectation for coeval systems. However, Chabrier *et al.* (2007) argued that such a phenomenon could be the result of preferentially strong magnetic activity on the primary that suppresses surface convection and that should also be manifested by the presence of large, cool surface spots. Chew *et al.* (2009) showed that a simple model with a small equatorial spot and a very large polar spot (covering fraction of $\sim$65%) could indeed reproduce the observed variations seen in the light curve and the different temperatures.

Recently, Stassun has summarized the current constraints on theoretical stellar models from the empirical measurements of the masses and ages of young low-mass stars and BDs (*e.g.*, Stassun *et al.* 2009). The main results of the comparison with the evolutionary models of Baraffe *et al.* (1998), D'Antona & Mazzitelli (1997), PS99, and Siess *et al.* (2000) are shown in Figure 2 and can be summarized as follows:

- Dynamical mass estimates are available for more than 30 PMS stars with mass $\lesssim$2 $M_\odot$, including single stars (from the rotation curve of circumstellar disks) and binary stars (both astrometric and eclipsing).

- Comparison to theoretical models in the HR diagram shows that above $\sim$1 $M_\odot$ there is a good agreement (both in mass and age) with a mean difference of 10% and a similar scatter, whereas below $\sim$1 $M_\odot$ the agreement is poorer with differences that can be as large as $\sim$100% and a large scatter.

- The best overall agreement is found with the models by Siess *et al.* (2000) and PS99: the overall consistency amounts to $\sim$5%, with a scatter of $\sim$25%.

- This agreement could be fortuitous and the models right for the wrong reasons (for example, by the effect of stellar activity on the effective temperatures that are ignored in the models). However, differences in track morphology are relevant, especially at M$\sim$0.5 $M_\odot$.

- Non-coevality of $\sim$40% is possible in low-mass binaries at $\sim$1 Myr. So, care must be taken in using coevality as a calibration for models.

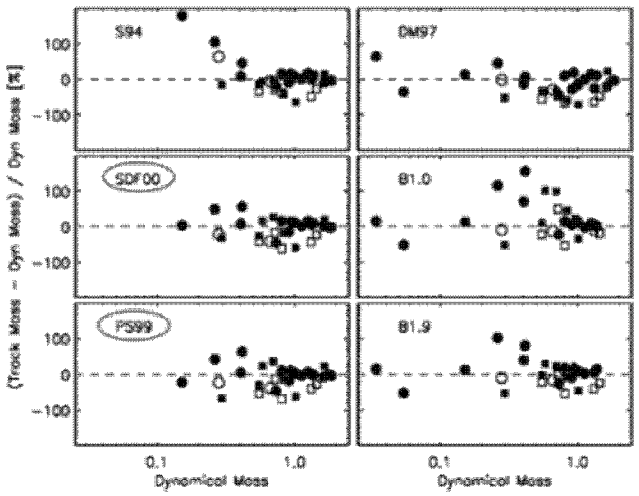

Fig. 2. Comparison of dynamical mass estimates of all known PMS binaries to theoretical models. (From Stassun 2010, priv. comm.)

The last point is particularly interesting since binaries are assumed to form coevally from the same material within dense cores. If this assumption is indeed correct, they represent a powerful calibration of evolutionary models (*e.g.*, Luhman 1999). In order to obtain an independent estimate of the degree of coevality of a large and uniform sample of binary stars, Kraus & Hillenbrand (2009) have presented a thorough study of the distribution in the HR diagram of all the known systems of Taurus-Auriga with spectral fluxes and flux ratios for at least two components. For the isochrones, they used the models of Baraffe *et al.* (1998) for low-mass stars ($M \lesssim 1.2\,M_{\odot}$) and D'Antona & Mazzitelli (1997) for more massive stars. Kraus & Hillenbrand found that the relative binary ages have an overall dispersion $\sigma \sim 0.40$ dex, while random pairs are coeval only to within $\sigma \sim 0.58$ dex. Thus, the binaries seem to be more coeval than the association as a whole. On the other hand, the distribution of relative ages indicates the presence of two populations: $\sim 2/3$ of the sample appears coeval to within the errors $\sigma \sim 0.16$ dex, while $\sim 1/3$ of the sample has a much wider age distribution up to 0.4–0.9 dex. As a possible explanation of this spread, Kraus & Hillenbrand suggest the presence of unrecognized hierarchical multiples, or stars seen in scattered light, or objects heavily contaminated by disk emission. They also find that the relative coevality does not depend on the system mass, mass ratio or separation. An enhanced coevality for the binary systems ($\sim 70\%$ of the sample) is consistent with the formation timescale of stars from individual dense cores and also gives credit to the adopted PMS isochrones used in the analysis.

3.2 Intermediate-mass stars

Information on the properties of intermediate-mass PMS stars, the so-called Herbig Ae/Be star, can come from eclipsing binary systems and from the unique feature

that on their way to the ZAMS, PMS stars with mass $1.5 \lesssim M/M_{\odot} \lesssim 4$ cross the pulsation instability strip in the HR diagram. This class of variable stars are called PMS δ Sct stars (*e.g.*, Ripepi 2006; Zwintz 2008). The relation between the pulsation period and the intrinsic stellar parameters (L, $T_{\rm eff}$) allows us to obtain independent information on the evolutionary properties and in particular on the stellar mass. Moreover, asteroseismological techniques can be applied to infer the internal structure of the observed pulsators. In the following, we will discuss some of the most recent developments on these topics and on the possible constraints on the initial conditions of PMS evolution, starting from the fortunate coincidence that a particular system, RS Cha, is both an eclipsing binary *and* a pulsating system.

3.2.1 The instability strip for intermediate-mass PMS stars

The first theoretical investigation of the PMS instability strip based on nonlinear convective hydrodynamical models was carried out by Marconi & Palla (1998), who calculated its topology for the first three radial modes. They also found that the interior structure of PMS stars crossing the instability strip is significantly different from that of more evolved main sequence stars (with the same mass and temperature), even though the envelope structures are similar. Subsequently, Suran *et al.* (2001) made a comparative study of the seismology of a 1.8 $M_{\odot}$ PMS and post-MS star. These authors found that the unstable frequency range is roughly the same for PMS and a post-MS stars, but that some non-radial (g) modes are very sensitive to the deep internal structure. More recently, Grigahcene *et al.* (2006) produced a theoretical instability strip for PMS stars for the first seven radial modes, and Ruoppo *et al.* (2007) have derived an analytical relation between the large frequency separation and the stellar luminosity and effective temperature and developed a tool to compare theory and observations in the echelle diagram. Finally, using the ATON evolutionary code, Di Criscienzo *et al.* (2008) have computed standard (non-rotating) and rotating PMS models to produce adiabatic oscillation spectra covering an extensive grid of parameter space.

From the observational point of view, to date more than two dozens of pulsating Herbig Ae stars are known. The location of the instability strip in the HR diagram and the position of a sample of known δ Sct pulsators is displayed in Figure 3. The typical pulsation periods are in the range of several hours and amplitudes between hundredths and thousandths of magnitude. Multi-site campaigns (Ripepi *et al.* 2003; Bernabei *et al.* 2009), and space observations with the MOST satellite (*e.g.*, Zwintz *et al.* 2009) have provided us with good set of frequencies to be compared to observations. A fundamental contribution to the field is being provided by the data collected by the CoRoT satellite (*e.g.*, Baglin *et al.* 2007). Indeed, this satellite images the same region of the sky for about five months consecutively, allowing to observe relatively faint stars (up to V$\sim$15 mag) in its "exoplanetary field", with good precision and very high duty cycle. During the first long-term pointing of CoRoT imaged a region of the sky in the galactic anti-center where a few distant Star Forming Regions were present, thus allowing the possibility to discover new δ Sct PMS candidates.

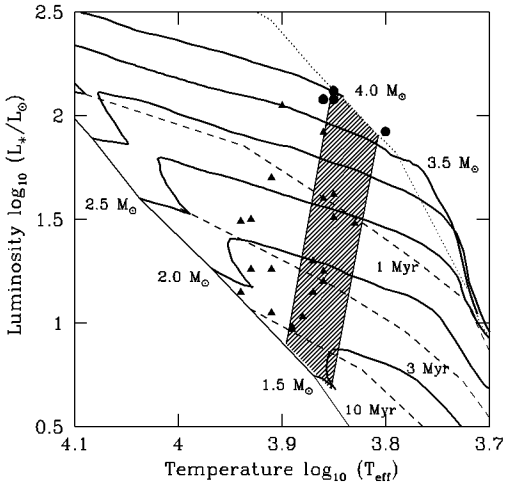

Fig. 3. The theoretical instability strip (dashed region) in the HR diagram, along with the position of a sample of known PMS δ Scuti pulsators. The filled dots are the stars that can be used to test the protostellar initial conditions, one of them being Lk Hα 349. (From Marconi *et al.* 2004.)

3.2.2 Pulsating stars: The case for RS cha

s A particularly illuminating case is provided by the star RS Cha, an eclipsing double-lined spectroscopy binary belonging to the young η Cha cluster. With a period of 1.7 days, it is an almost equal mass binary with $M_{\rm p} = 1.86\,M_\odot$ and $M_{\rm s} = 1.82\,M_\odot$ (Andersen 1991). The stellar parameters of both components place them inside or very close to the instability strip, making it the only δ Sct candidate known with this property. Recently, Alecian *et al.* (2005) presented resolved radial velocity curves showing evidence for pulsations with periods of the order of 1 hr which they interpreted as the signatures of δ Sct-type pulsations. Refinement of the mass determination yield values of $M_{\rm p} = 1.89 \pm 0.01\,M_\odot$ and $M_{\rm s} = 1.87 \pm 0.01\,M_\odot$ and a surface metallicity value $Z = 0.028$. Interestingly, the inferred stellar parameters could not be reproduced simultaneously for both components using abundance ratios of solar composition, but only if carbon and nitrogen were depleted by a factor 0.6 and 0.5 dex, respectively, while keeping the global metallicity unchanged (Alecian *et al.* 2007). A lower carbon abundance implies a weaker release of luminosity in the central regions due to the reactions $^{12}C \rightarrow {}^{13}C$ and $^{13}C \rightarrow {}^{14}N$ with a concurrent deacrease of the radiative gradient which delays the onset of a convective core. At the age of the system, $\sim$9 Myr, after the onset of the CNO cycle, the internal structure is particularly sensitive to any change in composition, thus revealing the power of seismological analysis for comparison to theoretical models. It is important to note that the lower C and N abundance is in agreement with the solar mixture derived by Asplund

et al. (2005) that predict lower abundances of these elements relative to Grevesse & Noels (1993).

Finally, we like to point out the recent discovery of non-radial pulsations in both components of RS Cha made by Böhm *et al.* (2009) using quasi-continuous, high-resolution spectroscopic observations during 14 nights. From the line profile variations in the primary and secondary components, the authors were able to derive two and three pulsation frequencies, respectively. The dominant mode of the primary appears to be a high degree prograde mode with $l = 10$ or 11, while that of the secondary is a low degree mode with $l = 0, 1$ or 2. These findings put further strong constraints on the internal structure of the star: it is clear that asteroseismology has become a viable tool for PMS stars too!

3.2.3 Pulsating stars: A test to the initial conditions of PMS stars

We now turn our attention to one of the four objects of Figure 3 located in the upper part of the instability strip, near the birthline. Unlike the case of the RS Cha system whose age of $\sim$9 Myr is such that the stars have completely lost memory of the initial conditions, stars in this part of the diagram have just completed their main accretion phase and are in the appropriate mass range ($\sim$3–4 $M_{\odot}$) where theory predicts a strong re-arrangement of the internal structure (Palla & Stahler 1993). In particular, such stars undergo a process of internal relaxation in which the internal convection disappears and the luminosity trapped during the accretion phase is finally liberated at the surface. In principle, asteroseismology on these stars should be capable of distinguishing between different internal structures, thus setting strong constraints on the accretion history.

A remarkable candidate for pulsation studies is the star LkHα 349, the brightest star of the small cluster associated with the Elephant Trunk globule IC1396 A (*e.g.*, Reach *et al.* 2009). The globule is illuminated by an O6 star whose ionization front has probably induced the formation of a new generation of (proto)stars, as detected by the *Spitzer* saltellite. The present configuration of the globule comprises an ionized layer on the side facing the O star (bright in Hα emission), a dense bright rim (with strong PAH emission), and a high-opacity region corresponding to the molecular cloud. This dense region comprises a round head, centered on Lk Hα 349, with a hole in its center, and an extended trunk with several star forming sites. The central star, Lk Hα 349, is responsible for the central cavity and has a spectral type F9e, effective temperature of 6165 K, and a luminosity of $\sim$250 $L_{\odot}$ (Hernández *et al.* 2004). These values place it near the birthline (age $\sim$0.3 Myr), consistent with other indications of youth, such as the Hα line with P Cygni profile indicating a strong wind and high rotation rate ($vsini = 190\,\mathrm{km\,s^{-1}}$), near the breakup speed.

An interesting experiment is to compare the internal properties inherited during accretion with those of a PMS star of the same mass who started contraction from the standard Hayashi-type initial conditions. The resulting curves are shown in the upper panel of Figure 4. The figure highlights the remarkable difference between the track of a 4 $M_{\odot}$ star with protostellar initial conditions (lower curve)

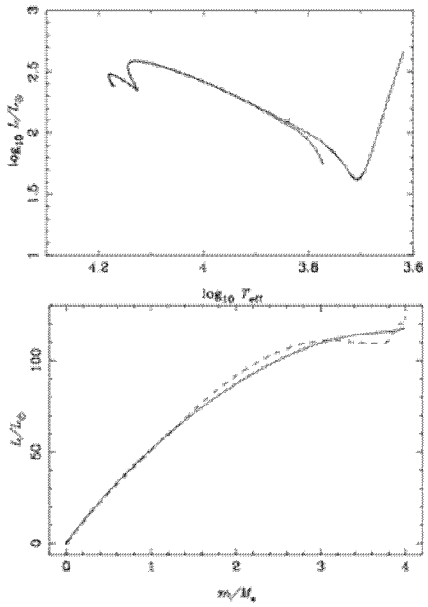

Fig. 4. *Top:* evolutionary tracks for a $4\,M_\odot$ star. The upper curve is for the standard initial conditions, while the lower curve is for the protostellar conditions. *Bottom:* the internal luminosity profile for the two models; the dashed curve is for the protostellar case. (Adapted from Marques *et al.* 2011.)

and the standard one (upper curve). The two curves join each other at a location near the red edge of the instability strip. The lower panel of Figure 4 displays the internal luminosity profile of the $4\,M_\odot$ star at the red edge: the solid and dashed lines are for the standard model and protostellar initial conditions, respectively. The latter corresponds to a thermally unrelaxed luminosity profile, while the former is characteristic of a fully radiative object. Now, the pulsation characteristics (periods, amplitudes) are particularly sensitive to the internal conditions, especially in the subsurface regions where the perturbations are excited. Detailed modeling indicate large differences in the excited linear and nonlinear modes that could be detected by future observations (Marques *et al.* 2011).

3.3 Massive stars: $M_* \gtrsim 8\,M_\odot$

What happens to massive stars? How can we test their mass and age from the location in the HR diagram? Is the accretion scenario developed for low- and intermediate-mass stars also valid for the most massive objects? Are very high accretion rates ($\dot{M}_{\rm acc} > 10^{-4}\,M_\odot\,{\rm yr}^{-1}$) really required? And, in case, is there evidence for an increase of $\dot{M}_{\rm acc}$ with mass? Since most massive stars are in clusters, are they the first or the last to form?

Our understanding of massive star formation is still very limited compared to that of solar-mass stars, for which a generally accepted theoretical framework exists. The roles of dynamical interactions and coalescence *versus* a more standard core and disk accretion framework are still debated (Beuther *et al.* 2007; Zinnecker & Yorke 2007). Considering the formation mechanism, it is clear that the accretion scenario that works well for lower mass objects has problems at the highest masses. The main one is that radiation pressure begins to become significant in protostars of intermediate mass. However, infall cannot be stopped as long as the accretion component dominates the total luminosity. It is known that for $\dot{M}_{\rm acc}\sim10^{-5}\,M_\odot\,{\rm yr}^{-1}$, a protostar joins the main sequence at a mass of $\sim8\,M_\odot$ where it releases $\sim3000\,L_\odot$, less than the luminosity delivered by H-burning ($\sim10^4\,L_\odot$) at that mass. Hence, the need for higher accretion rates (for example increasing with mass; see Maeder this volume), indirectly suggested by the large mass loss rates inferred from the associated outows. How to achieve the physical conditions for such high values of $\dot{M}_{\rm acc}$ is still not at all clear, although centrally condensed turbulent cores may serve the purpose (McKee & Tan 2003). Perhaps, the early suggestions of an entirely different mode of formation based on growth by coalescence of dense molecular cores (*e.g.* Stahler *et al.* 2000), or by accretion induced collisions and subsequent merging of protostars in the dense central regions of star clusters (*e.g.*, Bonnell *et al.* 1998) still represent viable alternatives.

In addition, progress in this field has been limited in part by the greater observational difficulties of studying massive protostars that are typically more distant, embedded, crowded and quickly evolving than their lower-mass counterparts. Orion is the closest star-forming region where young, massive ($\rm M\gtrsim8\,M_\odot$) stars are present, and as such is an ideal test case to study observationally and to understand theoretically. In the following, we will consider the interesting possibility offered by the special geometry around the KL object.

3.3.1 A case study: The massive source I in the Kleinmann-low nebula

Source I in the Orion-KL nebula is believed to be the nearest example of a massive star still in the main accretion phase. It is thus one of the best cases to study the properties of massive protostars to constrain high-mass star formation theories. Near-infrared radiation from source I escapes through the cavity opened by the OMC1 outflow and is scattered by dust towards our line of sight. Owing to the extremely high extinction along the line of sight, the direct observation of the source (photosphere or inner accretion disk) responsible for the high infrared luminosity of the Orion BN/KL nebula is precluded. However, the source can be indirectly seen through the scattered light of the surrounding bipolar nebula (Morino *et al.* 1998). Morino et al. obtained a $2\,\mu$m spectrum of the reection nebula tracing the radiation that escaped the dust surrounding the massive protostar possibly along the polar axis of a circumstellar disk. The spectrum shows absorption features due to CO ro-vibration bands formed at $\rm T\sim4500\,K$, while the inferred luminosity was estimated to be $\sim10^5\,L_\odot$. These features could be

interpreted as due to either a very large, cool massive protostar (radius $\gtrsim 300\,R_\odot$) or the "photosphere" of a very active accretion disk ($\dot{M}_{\rm disk} \gtrsim 4 \times 10^{-3}\,M_\odot\,{\rm yr}^{-1}$; *e.g.*, Nakano *et al.* 2000; Hosokawa & Omukai 2009).

In an attempt to resolve this issue and shed light on this interesting object, Testi *et al.* (2010) carried out intermediate resolutions (R$\sim$8900) near-infrared observations of the reflected spectrum from source I from Orion KL. They confirm that the absorption spectrum is generated close to the position of source I and scattered to our line of sight in the outflow cavity. However, it was not possible to find a good match for all the observed absorption features with a single photospheric template. It is likely that the Orion spectrum is produced by the combination of a wide range of photospheric temperatures, as in a very active accretion disk. The velocity dispersions implied by the absorption spectra, $\sigma \sim 30\,{\rm km\,s}^{-1}$, can be explained by the emission from a disk around a massive, $M_{\rm proto} \sim 10\,M_\odot$, protostar that is accreting at a high, $\dot{M}_{\rm acc} \sim 3 \times 10^{-3}\,M_\odot\,{\rm yr}^{-1}$, rate. The question, then, is whether such accretion disks are present around such massive protostars. A direct indication of their existence has been provided by the recent discovery of a compact disk around a $\sim 20\,M_\odot$ young stellar object with a molecular outflow and two bow shock perpendicular to the disk plane (Kraus *et al.* 2010).

3.3.2 Massive eclipsing binary systems

A distinguishing character of massive stars is their unusually high multiplicity, much higher than that of lower mass stars. While the binary frequency of solar-type stars is about 50% (*e.g.*, Duquennoy & Mayor 1991), and that of later spectral types is $\sim$10–15% (*e.g.*, Burgasser *et al.* 2003), for the more massive O- and B-type stars it exceeds $\sim$70% with a strong preponderance of very close systems (*e.g.*, Mason *et al.* 1998; García & Mermilliod 2001). The high multiplicity bears directly on the formation mechanism in which the peculiar physical conditions (high densities, both gas and stars) should be responsible for the observed ehnancement. Below, we will take advantage of this property to attack one of the remaining questions outlined at the beginning of the section: namely, whether massive stars form in a cluster at the same time as the lower mass siblings, or if there is evidence for a late birth. Ultimately, this question can be answered by assigning accurate ages, but since stars more massive than $\sim 8\,M_\odot$ are born on the main sequence, their ages cannot be determined by the usual methods of isochronal dating. However, well resolved, massive and young eclipsing binary systems with low-mass secondaries still in the PMS phase could in principle offer a unique way to circumvent this problem.

Indeed, eclipsing binaries provide very accurate stellar parameters through photometry and spectroscopy. For double-lined spectroscopy binaries, their light curves allow to obtain ratios of stellar radii which, combined with spectroscopy, can yield the physical radii and effective temperatures. On the other hand, velocity amplitudes determine mass ratios and the sum of the masses, so that individual masses can be obtained. Moreover, from the spectra one can derive effective temperatures, surface gravities, and luminosities. Finally, the reddening and distance can be obtained from the comparison of the luminosity and the observed brightness.

Thus, a complete characterization of the system can be performed with much higher accuracy than in the case of single massive objects. For example, the problem of the discrepancy between the mass derived from parameters determined from fitting atmospheric models to spectra and from evolutionary tracks does not exist in the case of eclipsing binary systems (see discussion in, *e.g.*, Bonanos 2009).

A very interesting case of multiplicity is provided by the Trapezium stars, the most massive objects of the Orion Nebula star forming cluster. Two of the four brightest Trapezium stars are eclipsing systems. The brightest star, Θ^1 Ori C is known to be a close visual binary system with a companion at a separation of 33 mas (corresponding to about 15 AU; Weigelt *et al.* 1999). By tracing the orbital motion of the system components over a period of a decade, Kraus *et al.* (2009) were able to determine a high eccentricity of the orbit (e∼0.6), a period of ∼11.3 yr, and total system mass of $44 \pm 7\,M_\odot$ (with a mass ratio $M_2/M_1 = 0.23$) at a dynamical distance of 410 ± 20 pc. More recently, Lehmann *et al.* (2010) have reported evidence for the presence of a third companion in a close eccentric orbit with a period of ∼62 days. By combining astrometric and spectroscopic information, they derive the absolute masses of the primary ($31 \pm 3\,M_\odot$), secondary ($12 \pm 3\,M_\odot$), and of the close third companion ($1.01 \pm 0.16\,M_\odot$). If this initial discovery is confirmed by future observations, the solar mass companion should be located well above the main sequence, in a position to allow an estimate of its isochronal age. However, determining the stellar properties of such a faint star is an observational challenge, since the light contribution of a one solar mass star is negligible compared to that of the more massive primary. Nevertheless, it is possible that in the future the weaker spectral lines will be detected, thus providing the desired information on the properties of the low-mass companion.

Returning to the eclipsing systems, BM Ori (= Θ^1 Ori B) and V1016 Ori (= Θ^1 Ori A), their properties have been studied in detail by several authors (*e.g.*, Schertl *et al.* 2003; Vitrichenko *et al.* 2006). Of particular interest is BM Ori, the least massive of the Trapezium stars, whose components (each a binary system) have a dynamical mass of $M_\mathrm{p} = 6.3\,M_\odot$ and $M_\mathrm{s} = 2.3\,M_\odot$, respectively. When placed in the HR diagram, the secondary falls very close to the birthline and the two stars align on the same isochrone for t∼1×10^5 yr, within the observational uncertainties (Palla & Stahler 2001). Thus, this somewhat massive system is very young, much younger than the average age of the cluster (∼2–3 Myr; see below). Such a young age could help explaining the so-called "proplyd conundrum" (*e.g.*, O'Dell 2001) related to the large number of proto-planetary disks (proplyds) observed in the Orion Nebula cluster and their short lifetimes. Since the UV radiation of the massive stars is responsible for their excitation, a young age would alleviate the problem and would lend further support to suggestions that massive stars tend to form relatively late in a cluster (for a different view on the simultaneous formation of massive stars and clusters, see Smith *et al.* 2009).

4 Clustered *vs.* isolated massive stars

The large majority of high-mass stars are part of stellar groups: young star clusters or OB-associations. This observation led to the idea that the formation of a

high-mass star is intrinsically connected to the formation of a star cluster. The two competing scenarios for the formation of massive stars, dynamical interactions and collapse from massive turbulent cores (*e.g.*, Bonnell *et al.* 1998; McKee & Tan 2003), make the common assumption that massive stars form inside a star cluster. However, a population of (apparently) isolated O-type stars is known to exist in the Galaxy. Some 70% of the O-type stars in the Galaxy are found in clusters or OB-associations, ∼10% are OB-runaway stars, and ∼20% are field O stars (Mason *et al.* 1998; Maíz-Apellániz *et al.* 2004). Then, the question is whether this non-negligible fraction of isolated stars is truly the result of formation in peculiar conditions or not.

In an attempt to elucidate the origins of isolated stars, de Wit *et al.* (2004, 2005) surveyed some 43 field O stars in the solar neighborhood with $V < 8^m$ classified as isolated in the catalogue by Mason *et al.* (1998) to search for undetected stellar clusters centered on the sample stars. The study revealed the presence of a well defined stellar density enhancement near the field O star in five cases (four of them previously unknown). Thus, the imaging survey revealed that ∼85% of the field O-type stars are in fact isolated. The low detection rate of star clusters leads one to consider the runaway star hypothesis as a possible mechanism for the origin of the field O stars.

Within a 2 kpc radius from the Sun, the percentage of confirmed O-type runaway stars is ∼10%. They are characterized by high spatial velocities (presently or in the past) acquired from dynamical interactions in the centres of young dense stellar clusters or due to a binary supernova explosion (*e.g.*, Blaauw 1961; Hoogerwerf *et al.* 2001). In order to evaluate the runaway nature for the eld O stars, de Wit *et al.* (2005) re-examined their spatial velocity distribution using Hipparcos data, their spatial distribution with respect to the Galactic plane, and their proximity to known young clusters. The study resulted in the identification of 22 new candidate runaways, reflecting the importance of dynamical interaction in young clusters. On the other hand, the fraction of the O-type stars not associated with a cluster/OB association was found to be $4 \pm 2\%$ (12 O stars). Among these stars, only one is a confirmed spectroscopic binary and two are suspected visual binaries. Thus, unlike the majority of O-type stars that are part of binary/multiple systems (as discussed before), the presence of a small fraction of genuine isolated stars indicated a further peculiarity in their formation process.

However, a Monte-Carlo simulation aimed at estimating the probability of forming massive stars in isolation, assuming that all massive stars are formed in clusters that are distributed in size according to a power law (*e.g.*, Oey *et al.* 2004) down to "clusters" of a single star, shows an interesting result. Indeed, the observed fraction of isolated stars is expected if the slope of the cluster mass function (CMF) is $\beta = -1.7$, largely independent of the shape of the stellar IMF. Interestingly, a similar slope of the CMF is also required to explain the cluster richness of Herbig Ae/Be clusters due to IMF and CMF sampling (Testi *et al.* 1999; Bonnell & Clarke 1999). On the contrary, the commonly adopted value of $\beta = -2$ observed in the solar neighborhood (Lada & Lada 2003) would predict too many single O-type stars and too many clusters with only one O-type star. The

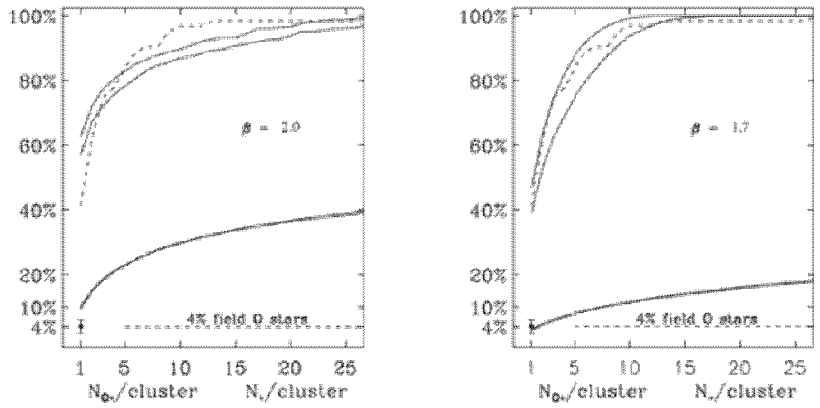

Fig. 5. The cumulative distribution for the total number of stars per cluster (lower full curves) and the number of O-type stars per cluster (upper full curves). The dashed curves correspond to observed number fraction for Galactic OB-associations. The observed number of Galactic eld O-type stars is indicated by the point with errorbar. The left panel is for a CMF with slope $\beta = -2.0$ and the right panel for $\beta = 1.7$. The latter fits the observations. (From de Wit *et al.* 2005.)

resulting distributions are shown in Figure 5. However, Parker & Goodwin (2007) reanalyzed this issue and found that, by assuming an isolated O star as being an O star without B-type star companions and allowing for the presence of a cluster of low-mass stars with a mass $<100\,M_{\odot}$, they could reproduce the small fraciton of isolated stars with a CMF slope of -2.

In conclusion, although in rare occasions, it appears that the Galaxy is able to form a single massive star without the requirement of a stellar cluster. More recently, Pflamm-Altenburg & Kroupa (2010) have proposed that the small fraction of isolated stars can be the result of a two-step ejection process in which a massive binary is dynamically ejected from a star cluster as a result of close encounters between binaries and single stars or binaries and binaries with subsequent supernova explosion of one binary component with recoil of the other binary component. In this way, even the apparently isolated field stars may owe their origin to a crowded environment.

5 The initial mass function

Any attempt to understand the origin of stellar groups must address the issue of their mass distribution. It is not obvious that any single function should adequately describe all existing systems. In principle, the natural variation in such environmental factors as the ambient magnetic field, the level of turbulence, or the molecular cloud temperature prior to cluster formation could yield a wide

variety of distributions. However, the empirical information from detailed studies of galactic star forming regions is that massive stars are intrinsically rarer than their low-mass counterparts. In fact, this property appears to hold in galaxies of the local universe observed at sufficient resolution to resolve the low-mass population, and the general consensus is that it has a universal significance. We present here some recent developments in the determination of the initial mass function (IMF), starting from some historical notes.

5.1 A bit of background

It is instructive to briefly revisit the approach followed by E.E. Salpeter in his derivation of the IMF (see Salpeter 2002 for a vivid account). First, the motivation to look into this fundamental issue came from the need to prepare a table containing all the properties of main-sequence stars as a function of mass for a book on *Energy production in stars* that however was never published. Such data were not fully available at the time (1954) and in order to obtain them, some extrapolations and guesses were necessary. The astrophysical question behind the table was the lack of knowledge about the amount of enrichment of the interstellar gas due to the explosion of massive stars, considering that such objects are very rare at present times. This question was important since just a year earlier Burbidge, Burbidge, Fowler and Hoyle had shown that the heavy elements are synthesized in the interior of massive and very massive stars and subsequently released into the interstellar medium after supernova explosions (Burbidge *et al.* 1957) . In addition, the concept of two stellar populations had been introduced by Baade with the assumption that stars had been forming continuously over the lifetime of the Galaxy (estimated then at $\sim$6 Gyr).

Then, the relevant question was how many massive stars were born and had died over the lifetime of the Galaxy. In order to answer it, a calculation of the *initial mass function*, or *birthrate function* was necessary. In order to do that, several assumptions had to be made that required the knowledge of: the lifetime of a star as a function of mass, the mass-luminosity relation, and the luminosity distribution of Population I stars. It is interesting to note that Salpeter, unlike other prominent scientists of his time (in particular, G. Gamow), did not believe that the birthrate of massive stars (the heavy element producers) was negligibly small over the last $\sim$6 Gyr of the life of the Galaxy.

For the calculation, Salpeter made three important assumptions (*chuzpah*, or wild guesses): ignore the mass dependence of the star distribution perpendicular to the galactic disk, assume that the absolute rate of star formation is constant over 6 Gyr (T_0), and, most importantly, assume that for brighter Population I stars the total Initial Luminosity Function (ILF) is larger than the observed LF by the factor T_0/τ_{MS}, where the latter term is the (by then) hypothetical lifetime of a star of mass M after leaving the main sequence. Salpeter estimated that $\tau_{MS} = 0.12 \times \tau_H(MS)$, where the $\tau_H(MS)$ is the hydrogen burning time on the main sequence, a known quantity. The result was a simple expression for the IMF as a power-law with exponent -2.35, if defined per unit mass (Salpeter 1955). In

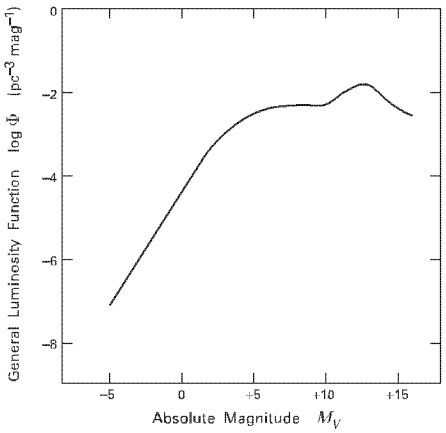

Fig. 6. Luminosity function for stars in the solar neighborhood. (From Stahler & Palla 2004.)

addition, Salpeter was able to calculate that the mass of all stars that have formed almost equals (∼80%) the mass in existing stars, thus implying that massive stars are indeed very important, and that the number of stars that have died is ∼12% of the number of existing stars. Since the notion of neutron stars or black holes was still lacking, the dead stars were identified as white dwarfs, whose fraction is indeed about 10%.

5.2 Current parametrizations for the IMF

Here, we first present a derivation of the IMF for field stars in the solar neighborhood. Then, we will compare it with mass functions derived in SFRs and young clusters and show that the two mass distributions resemble each other, at least approximately. The first point to underline is that, even for an unobscured field star at a known distance, its mass is not a quantity directly observable (apart from members of the rare eclipsing binary systems), but rather it is the luminosity within a certain wavelength range. A fundamental statistical property of field stars is the *luminosity function*, $\Phi(M_V)$. This function is defined so that $\Phi(M_V)\,\Delta M_V$ is the number of stars per cubic parsec in the solar neighborhood with absolute visual magnitude between $M_V - \Delta M_V/2$ and $M_V + \Delta M_V/2$. Its current representation is displayed in Figure 6.

The main properties of the luminosity function can be summarised as:

- The LF rises with increasing M_V up to $M_V \approx +12$, indicating that there are more faint than bright stars in any fixed magnitude interval.
- The LF levels off at about $M_V^* = +5$: this transition corresponds to stars whose MS lifetime is similar to the age of the galactic disk ($t_{\rm gal} = 1\times10^{10}$ yr).

- The origin of the change in slope is due to the fact that low-mass stars with $M_V \gtrsim M_V^*$ have been accumulating steadily over the lifetime of the Galaxy, while only a fraction of the brighter, short-lived stars with $M_V \lesssim M_V^*$ have survived.
- The turnover above $M_V \approx +12$ reflects the decrease in the occurrence of very low-mass stars and BDs, although its reality is still affected by uncertainty in the correction due to binary systems.

In order to transform the LF given above into the true initial LF, one must correct for the relative production of stars of different magnitude. Let $\dot{m}_*(t)$ be the total Galactic star formation rate per square parsec near the solar position. Then, the ILF, $\Psi(M_V)$ represents the relative frequency with which stars of a given M_V first appear and is normalized to unity: $\int \Psi(M_V)\, dM_V = 1$. If we set M_V^* to that magnitude for which $t_{\rm MS} = t_{\rm gal}$, the luminosity function can be written as an integral over time, where the integration limits depend on M_V and where one has ignored the possible time-dependence in $\Psi(M_V)$ or in the scale height $H(M_V)$:

$$\Phi(M_V) = \begin{cases} \int_{t_{\rm gal}-t_{\rm MS}}^{t_{\rm gal}} dt\, \dot{m}_*(t)\, \Psi(M_V)\, [2\, H(M_V)]^{-1} & \text{if } M_V < M_V^* \\ \int_0^{t_{\rm gal}} dt\, \dot{m}_*(t)\, \Psi(M_V)\, [2\, H(M_V)]^{-1} & \text{if } M_V \geq M_V^*. \end{cases} \tag{5.1}$$

Since the MS lifetimes $t_{\rm MS}(M_V)$ are known, one can invert Equation (5.1) and obtain $\Psi(M_V)$, *provided* the star formation rate $\dot{m}_*(t)$ is also known. For example, one can assume a constant value of $\dot{m}_*(t)$, since the final result is rather insensitive to the adopted functional form.

Once $\Psi(M_V)$ has been derived, the last step is to obtain the IMF, $\xi\,(M_*)$, *i.e.* the relative number of stars produced per unit mass interval. Normalizing this function to unity, the IMF is:

$$\xi\,(M_*) = \Psi(M_V) \frac{dM_V}{dM_*}. \tag{5.2}$$

The derivative on the righthand side represents the mass-luminosity relation on the main-sequence, whose functional form is empirically well known ($\mathrm{L} \sim M^\alpha$, with $\alpha \gtrsim 3$). Since $\mathrm{M}_V \sim \log \mathrm{M}$, it is $\mathrm{M}_V \sim \log \mathrm{M}$. Then, the IMF is defined per unit logarithmic mass interval as $\mathrm{M}_* \xi(M_*)$: $\xi\,(\log M_*) \sim \mathrm{M}^{-1.35}$, or $\xi\,(M_*) \sim \mathrm{M}^{-2.35}$ per unit mass. The latter is the original derivation of the Salpeter IMF.

Of course, this simple derivation of the IMF must be replaced by a more accurate treatment of the various simplification made so far. One of the most frequently used parametrisations is that proposed by Kroupa *et al.* (1993) where for convenience the IMF is approximated by a three-segment power-law:

$$\xi\,(M_*) = \begin{cases} k\,(M_*/M_\odot)^{-1.2} & 0.1 < M_*/M_\odot < 1.0 \\ k\,(M_*/M_\odot)^{-2.7} & 1.0 < M_*/M_\odot < 10 \\ 0.40\, k\,(M_*/M_\odot)^{-2.3} & 10 < M_*/M_\odot \end{cases} \tag{5.3}$$

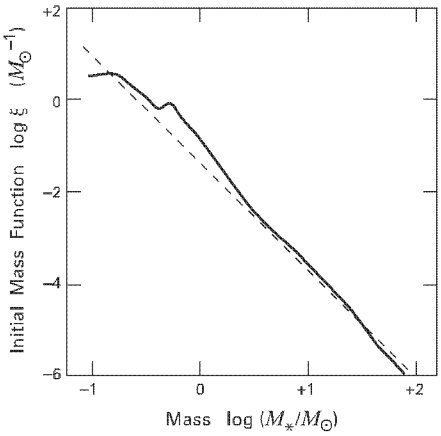

Fig. 7. The IMF for stars in the solar neighborhood. The dashed line has the slope −2.35, as in Salpeter. (From Stahler & Palla 2004.)

where k is a normalization constant. Figure 7 depicts Kroupa's IMF, showing a distribution flatter than Salpeter's below $\sim 1\,M_\odot$ and approaching it for masses $\gtrsim 5\,M_\odot$. However, the important message of the IMF is that half of all stars are produced with $M_* \geq 0.2\ M_\odot$. Only 12 percent have masses exceeding $1\ M_\odot$, while the fraction drops to 0.3 percent for stars above $10\ M_\odot$. Conversely, 70 percent of stars have $M_* \geq 0.1\ M_\odot$. Thus, the main conclusion is that *the star formation process yields objects with a characteristic mass of a few tenths of* $M_\odot$.

More recently, Weidner *et al.* (2010) have proposed a multicomponent power-law IMF with exponents that differ from the previous ones as they have been corrected for unresolved multiple systems. The exponents of the IMF are: −0.3 for $0.01 < M_*/M_\odot < 0.08$; −1.3 for $0.08 < M_*/M_\odot < 0.5$, and −2.35 for $1 < M_*/M_\odot$. Accordingly, the IMF has a two-part power-law in the stellar regime, while matching Salpeter IMF for stars greater than ∼solar. As a result, BDs contribute only about 4% by mass. A log-normal form of the IMF below $\sim 1\,M_\odot$ and a power-law extension to high masses has been suggested by Chabrier (2003): its shape is remarkably similar to the prescription by Kroupa and collaborators. Finally, a further parametrization of the IMF has been suggested by De Marchi *et al.* (2005) with a tapered power-law form

$$f(M) = \frac{dN}{dM} \propto m^{-\alpha} \left[1 - e^{(-m/m_c)^\beta}\right] \tag{5.4}$$

where m_c is the characteristic (or peak) mass, α is the exponent of the power-law for the upper end of the IMF, and β is the tapering exponent that describes the lower end of the distribution. As we will see below, this functional form reproduces well the IMF for clusters in SFRs, young open clusters and Galactic globular custers.

5.3 The IMF of young clusters and associations

Many recent reviews deal with this topic and there is no need to cover the large literature available on the empirical determination of the IMF in young clusters and associations. Useful references include the reviews by Zinnecker & Yorke (2007) and Bastian *et al.* (2010), as well as the monograph on the 50th anniversary of the publication of the IMF paper by Corbelli *et al.* (2005).

There are several advantages in measuring the IMF in star forming regions. In the first place, the accuracy is expected to be higher since once can apply observational tests to the models and there is no need to convert from present-day mass function to the initial MF. Also, all members of a complex have the same age and distance (although in some cases, significant spreads in both quantities are observed) and the completeness of the sample population is larger due to the fact that (a) both very low-mass stars and BDs are bright when young and (b) dynamical evolution and mass segregation are minimized. Finally, an important bonus is that the initial conditions are directly observable, rather than guessed.

On the other hand, a number of complications affect in a significant manner the determination of the fundamental stellar parameters (effective temperature and luminosity) that allow an estimate of mass and age through comparison with theoretical models. Among them: excess emission both in the UV and IR due to accretion and circumstellar disks that produce veiling in the spectra and that must be carefully accounted for in order to derive the stellar bolometric luminosity; the presence of significant amount of variable extinction; surface gravity effects that complicate the conversion from spectral type to temperature. In addition, the uncertainty in the theoretical models that we have discussed at the beginning introduce additional errors on the mass determination, typically at the 30–50% level (*e.g.*, Hillenbrand & White 2004). Finally, true membership is obviously needed and that requires good spectra for each individual object.

In spite of the difficulties, the most important SFRs in the solar neighborhood have been extensively surveyed, mainly to probe the low-mass end of the IMF, and some common results have emerged. Obviously, one of the best studied case is the Orion Nebula Cluster, but we defer to Section 7 for a derivation of the IMF. Other studies include Taurus-Auriga, Chamaeleon I and II, IC 348, NGC 1333, σ Ori, ρ Ophiuchi, and η Cha (*e.g.*, Alcalá *et al.* 2008; Burgess *et al.* 2009; Luhman 2007; Luhman *et al.* 2009; Lodieu *et al.* 2009; Marsh *et al.* 2010; Scholz *et al.* 2009). The main results can be broadly summarised as follows:

- The IMF is populated by objects which continuously span a range of mass, from the most massive stars to substellar objects near the deuterium burning limit (DBL = $0.012\,M_{\odot}$).
- The IMF is characterized by a broad peak near $0.2\,M_{\odot}$, suggesting a characteristic mass for star formation near 0.2–0.3 solar masses.
- Substellar objects account for only 20–25% of all sources produced by the IMF. The IMF declines from the HBL to the DBL. BDs are found down to $\sim 5\,M_{\rm Jup}$. Freely floating objects of planetary mass are very rare.

- The IMF appears universal in form, at least within the uncertainties inherent in the measurements.

The only significant variation in the IMF is found in Taurus that shows a remarkable surplus of stars with spectral type K7–M1. All the other SFRs have distributions that peak around a spectral type M5. As to the properties of the substellar IMF, theoretical models weakly dependent on the Jeans mass through dynamical interactions (*e.g.*, Bonnell *et al.* 2007) predict results consistent with the observed distributions. Remarkably, the lack of strong variations of stars to BD ratio is a problem for gravoturbulent models of cloud fragmentation and collapse, as they predict strong variations in the IMF as function of the Mach number and density and a shift of the IMF peak at higher masses in regions of low turbulence (*e.g.*, Padoan *et al.* 2007). On the other hand, recent models based on gravothermal and gravoturbulent collapse appear to reproduce well the shape of the IMF (*e.g.*, Hennebelle & Chabrier 2008, 2009).

5.4 Final considerations

Extending the discussion to slightly older, but still young (in galactic evolution terms) open clusters, the IMF has been determined in a number of systems of increasing age down to the substellar regime. These systems include NGC 2547 (∼30 Myr; Jeffries *et al.* 2004); IC 4665 (∼30 Myr; de Wit *et al.* 2006); α Persei (90 Myr; Barrado y Navascués *et al.* 2002); Blanco I (120 Myr; Moraux *et al.* 2007); and the Pleiades (125 Myr; Lodieu *et al.* 2007). Taking the IMF of the Pleiades as a benchmark, thanks to the depth and accuracy of its derivation, most clusters show similar properties characterized by log-normal distributions with characteristic mass of $\sim$0.2–0.3 $M_\odot$ and modest evidence for mass segregation. The latter becomes more prominent in older systems as a result of significant dynamical evolution. This is the case for the Hyades (625 Myr; Bouvier *et al.* 2008) and the similarly aged Praesepe (590 Myr; Kraus & Hillenbrand 2007: Boudreault *et al.* 2010).

Evidence for a variation of the field stars (Kroupa/Chabrier) IMF in older open and globular clusters mainly ascribable to their dynamical evolution is clearly shown in the comparative analysis of De Marchi *et al.* (2010) shown in Figure 8. These authors find that the present-day stellar mass function of large sample of clusters can be well represented by a tapered power-law with an average value of the index $\alpha = -2$, $\beta = 2.5$ (consistent with Salpeter), and a characteristic mass m_c in the range 0.1–0.8 $M_\odot$. Quite remarkably, the mass distribution does not appear to depend on the total cluster mass and central condensation, whereas, as expected, a definite correlation with the dynamical age is found.

In conclusion, the canonical IMF is understood as an invariant Salpeter power-law slope above $\sim$0.5 $M_\odot$, independent of the cluster density and metallicities for metallicities Z $\gtrsim$0.002 (*e.g.*, Massey & Hunter 1998; Pflamm-Altenburg & Kroupa 2006). This remarkable result on the apparent universality of the IMF lends much credit to the original derivation by Salpeter. However, it is useful

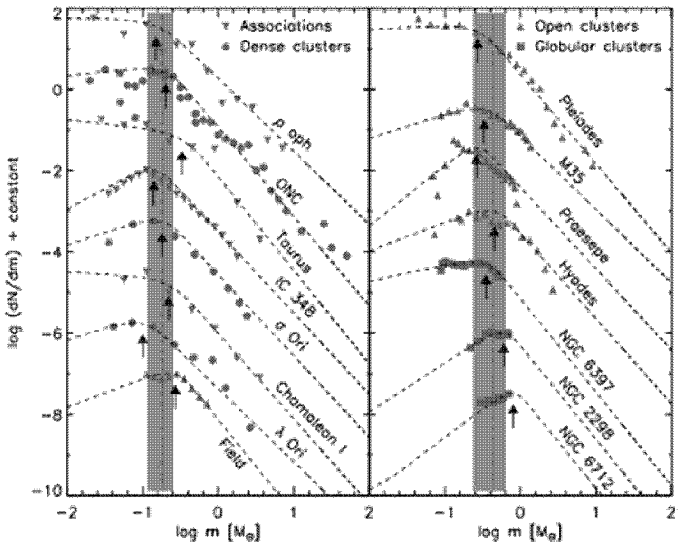

Fig. 8. The present day mass function for star forming regions, young and evolved open clusters, and globular clusters. The dashed lines are the fit using the tapered IMF with the characteristic mass m_c indicated by the arrows. The dashed regions display the standard deviation of m_c. Note the expected shift in the value of m_c for older systems. (From Bastian *et al.* 2010.)

to remind a remark made by Salpeter in his 2002 review "*Developments (or lack thereof) in the 45 years since have been good for me personally, but bad for science: I had hoped that my IMF was only an average for today and that the actual function would vary strongly from quiescent to active regions and would also vary from the young galaxy to the galaxy today.*"

6 Ages and age spreads in SFRs and young clusters

6.1 The physical motivation: Duration of star formation

The problem of the origin of stars is obviously directly linked to the question of what supports a massive cloud against its self-gravity before the production of an interior stellar group: how do individual dense cores, each capable of forming single and binary stars, arise within the magnetized and turbulent medium that characterizes molecular clouds? Answering the above questions requires a broader understanding that is currently at hand, one that connects the birth of individual stars to the growth and evolution of clouds on a multiparsec scale. A big effort in this respect is represented by a variety of numerical simulations of cloud evolution and star formation based on gravoturbulent (*e.g.*, Ballesteros-Paredes *et al.* 2007)

or MHD turbulent (*e.g.*, Kritsuk *et al.* 2009) models. In simple terms, the picture that emerges from these models is one in which molecular clouds are formed in large-scale turbulent HI flows and that the intersection of these flows compresses the gas to the point that it collapses, fragmenting simultaneously into stars over a broad front (*e.g.*, Hartmann *et al.* 2009). Star formation is thus considered as a process that occurs promptly in localized regions where turbulence is dissipated in a dynamical timescale (Elmegreen 2000). Then, molecular clouds can sustain star birth only for few million years.

This dynamic picture contrasts sharply with that suggested by, *e.g.*, Palla & Stahler (2002) in which the formation of dense cores is not seen as a random event in the cloud medium, but is supposed to occur in response to some global change in that medium. One such change would be large-scale, gravitational contraction of the parent cloud. This contraction presumably occurs through gradual loss of the mechanical support driven by ambipolar diffusion, *i.e.* the clouds evolve in a quasi-static fashion (Mouschovias *et al.* 2006). The time scale for this process is of order of $\sim$10 Myr and exceeds that predicted by the dynamic models (Krumholz & Tan 2007). Empirical evidence in favour of the slow mode of star formation comes from the reconstruction of the star formation history in clusters and associations using the classical method of placing stars in the HR diagram to infer isochronal ages. The application of this method to the most conspicuous regions in the solar vicinity with a statistically signicant population of young stars has led to the following conclusions (Palla & Stahler 2000). In general, it is found star formation began at modest levels roughly 10^7 yr in the past and increased rapidly toward the present epoch with an acceleration pattern. This trend is similar in different systems, although the time scale of the acceleration varies from region to region, typically 1–3 $\times$ 10^6 yr. The fast acceleration must be followed by a prompt deceleration to limit the global star formation efficiency of each unit to the observed low values (few percent). Evidence for such a steep decline is seen in regions such as Upper Scorpius and σ Ori where the activity reached a peak $\sim$3 $\times$ 10^6 yr ago and then dropped essentially to zero owing to the efficient removal of the dense gas by the radiative and mechanical effects of while additional discussion is provided by Palla (2004).

It is important to note that the two models of fast and slow star formation share the same property of a pattern of star birth accelerating with time, but they depart in an essential respect: in the dynamic mode there is no past activity and star formation occurs in a single major burst, while in the quasi-static mode there is a long history that can be traced back to its beginnings.

6.2 Age dating: Methods

How can then one hope to measure ages in clusters and associations at a level of distinguishing between the two views on the duration of the star formation process? There are various theoretical methods that provide an answer, including the location in the HR diagram or in extinction-corrected color-magnitude diagrams in comparison to isochrones; depletion of light elements (*e.g.*, lithium)

during PMS contraction; stellar pulsation. On the other hand, empirical diagnostics for age-dating stars rely on stellar rotation, chromospheric (Hα, Ca II H&K) and coronal (X-rays) activity, Li-depletion trend, age-metallicity and age-velocity dispersion relations. Most of them depend not only on age, but also on mass and that introduces an extra complication in the analysis. None of them is particularly sensitive to young ages, so that obtaining absolute ages is very difficult and highly uncertain in any case.

The presence of a relatively old population in young clusters and associations seems to indicate that molecular clouds can produce stars over extended periods ot time. Whether the inferred age spread is real or not is the central question to be answered. Although much information is available from the study of regions of ongoing star formation, a definite answer cannot come from them since they are still actively turning dense gas into stars and we cannot infer how long this process will continue in the future. Thus, active SFRs can only provide a lower limit to the true age spread.

In contrast, the ideal laboratories to derive reliable age spreads are represented by two other classes of objects: fully exposed, young clusters and associations (t $<$ 10 Myr), and intermediate-age (t$\sim$10–30 Myr) open clusters. In both cases, the key to determine their age and age spread is the use of the lithium depletion history and boundary tests (LDB) as a powerful clock (*e.g.*, Basri *et al.* 1996). This method is well known to the stellar community for its successful application to a number of older open clusters, such as α Per, IC 2391, NGC 2547, and the Pleiades, with significant revisions of their ages (*e.g.*, Jeffries 2004). In the remaining part of the section, we will discuss the potential of its application to younger systems.

6.2.1 The lithium test

Empirically, the presence of a strong Li I line at 6707.8 Å is an indication of youth in late-type stars. The observed regularity of the pattern of lithium depletion in open clusters of different ages indicates that this diagnostic can be used as a mass-dependent clock (Jeffries & Naylor 2001). Therefore, the combination of the measurement of the lithium equivalent width in high resolution spectra and the estimate of the abundance through the use of accurate model atmospheres and theoretical evolutionary models offers a powerful way to obtain reliable stellar ages.

The lithium test rests on the ability of young stars and brown dwarfs to deplete their initial lithium content during the early phases of (PMS) contraction. Young, low-mass stars ($M_* < 1\,M_\odot$) begin their PMS phase with the full interstellar supply of lithium since the central regions are too cold to ignite nuclear burning during the protostellar phase. As contraction proceeds, the critical temperature for lithium reactions ($\sim 2.5 \times 10^6$ K) is reached, and the initial content is readily depleted in fully convective, sub-solar stars ($M_* < 0.5\,M_\odot$). Even brown dwarfs with mass $\gtrsim 0.065\,M_\odot$ can attain central temperatures high enough for Li-burning (*e.g.*, Basri 2000). It has been shown that the physics required to study the depletion history as a function of age has little uncertainty, since it depends only on the stellar mass and radius (*e.g.* Bildsten *et al.* 1997). These

authors also derived simple and accurate (better than ∼20%) relations for the time variation of the luminosity (their Eq. (4)) and for the amount of Li depletion at a given age (their Eq. (11)) for fully convective objects undergoing gravitational contraction at approximately constant effective temperature and assuming fast and complete mixing. From the observed luminosity and effective temperature, one can then construct a plot of the mass depletion time relation that is bounded by the determination of the Li abundance.

According to models, fully convective stars in the range 0.2–0.5 $M_{\odot}$ start to deplete lithium after about 2 Myr, and completely destroy it in approximately 10 Myr (*e.g.*, Baraffe *et al.* 1998). Lower mass stars take much longer to burn lithium, and there is a sharp transition (*i.e.*, the boundary) between fully depleted objects and those with the initial lithium content. The mass at which the boundary occurs reveals the age of the cluster. Stars more massive than $\sim 0.8\,M_{\odot}$ only burn a small fraction of the interstellar value; on the other hand, fully convective objects ($M_{*} < 0.5\,M_{\odot}$) readily consume lithium while contracting toward the ZAMS.

Returning to the criteria for selecting suitable astronomical objects, the choice of open clusters with ages between 10 and 30 Myr is dictated by at least three reasons. First, by this time the star formation activity is certainly completed. Second, the age spread can be better estimated than for older systems since isochrones at this age do not suffer from crowding. Third, the LDB falls in the stellar regime (between 0.2 and 0.4 $M_{\odot}$ for typical distances) and thus can provide strong constraints on their internal structure. So far, the LDB test has been determined in older systems where it falls in the substellar regime. The identification of the best systems to study is not easy, due to an intrinsic paucity of open clusters of the appropriate age in the solar vicinity.

The other class of fully exposed, young clusters and associations may be considered at first sight a surprising choice since one would not expect to see any feature related to lithium burning and depletion. However, several studies have shown that this is not true in general, as in the case of the Orion Nebula Cluster, σ Ori, and Taurus-Auriga, as we shall see below.

6.2.2 Li-depletion in young clusters/associations

The first evidence for lithium depletion in a young star was presented by Song *et al.* (2002) for the binary system HIP 112312, a likely member of the β Pic moving group. Interestingly, while the primary star (spectral type M4) showed no lithium feature, the strong Li 6708 Åabsorption line was seen in the secondary (∼M4.5), a clear sign for the Li-depletion boundary (LDB). Using theoretical models, Song *et al.* derived a nuclear age $\gtrsim$20 Myr, higher than the isochronal age of ∼12 Myr (Zuckerman *et al.* 2001). An even stronger inconsistency between the two ages was found by White & Hillenbrand (2005) in the case of the star St 34 in Taurus-Auriga whose position in the HR diagram indicated an age of 8 ± 3 myr vs. a nuclear age of $\gtrsim$35 Myr.

Recently, Yee & Jensen (2010) have presented an extended analysis of the lithium abundance of several low-mass members of the β Pic moving group (spectral type K5 to M4.4) finding several fully Li-depleted stars, but no evidence for the LDB even in the latest-type members (M5), an indication that Li-depletion occurs

at a faster rate than predicted by the stellar models. The authors also found the same inconsistency between the nuclear and isochronal ages with models predicting less lithium depletion than observed. As a possible solution to the discrepancy, Yee & Jensen suggest that the actual radii of the M-type stars are larger than those predicted by the models (see also Torres *et al.* 2006). Macdonald & Mullan (2010) have suggested that the inclusion of a specific treatment of magneto-convection in low-mass models can change both the isochrones and the rate of Li-depletion in a significant manner, depending on the extent of the convection region and on the ionization state of the plasma. However, in order to reconcile the two estimates, the stars of the β Pic group should have an age of $\sim$40 Myr, a factor of two older than previous values (21 ± 9 Myr, Mentuch *et al.* 2008).

Lithium abundances have been obtained in several well known young clusters, including Taurus, σ Ori and the ONC. The main result is that, despite their young average ages ($\sim$1–3 Myr), several Li-depleted stars have been discovered in all of them (Palla *et al.* 2005, 2007; Sacco *et al.* 2007; Sestito *et al.* 2008). The case for the ONC is particulary interesting owing to the presence of several bona-fide members (membership probability higher than 90%) with Li abundances well below the interstellar value (factors of $\sim$5 to >100), although the vast majority of the other ONC members do not show any evidence for Li-depletion consistent with their young average age. The comparison of the Li-depleted stars with the analytic prescriptions of Bildsten *et al.* (1997) are shown in Figure 9. The nuclear age and mass can be read off by the intersection of the two curves (and the shaded region gives the theoretical uncertainty), while the mass and age estimates from the HR diagram are given by the points. As one can see, in four cases the agreement between the two estimates is excellent (at the level of a few percent), whereas in two cases the nuclear age is much larger than the other (similar to the case for the β Pic group). It is important to stress that the derived ages of about 10–20 Myr indicate that the ONC does contain objects much older than the average age of the dominant population. Thus, the star formation history of the ONC extends long in the past, although at a reduced rate, in accordance with the empirical evidence found in the majority of nearby clusters and associations (Palla & Stahler 2000) and, as we shall see below, with the results of a recent analysis of the population of the ONC that confirms the large spread in luminosity (hence, age) originally found by Hillenbrand (1997). This empirical finding is supported by theoretical considerations on the formation of clusters via quasi-equilibrium configurations over several (3–5) dynamical times (Tan *et al.* 2006; Huff & Stahler 2007). For a different view in which the apparently older population of star clusters can be due to capture during the formation phase of the underlying older population, thus saving the idea of a short-lived, highly dynamical process, see, *e.g.*, Pflamm-Altenburg & Kroupa (2007).

6.2.3 LDB in young open clusters

A large effort has been done in the past on open clusters, comparing the cluster age derived from the LDB in the lowest-mass stars to the isochronal age from a

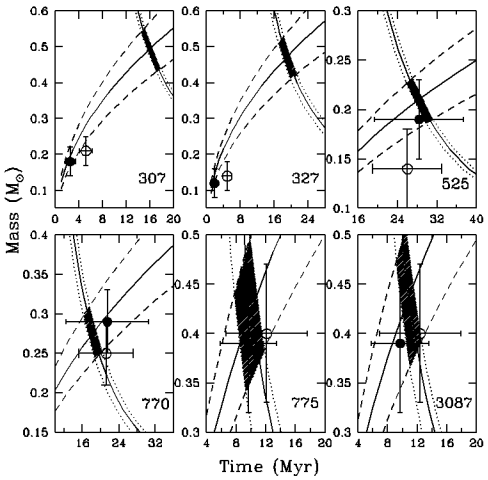

Fig. 9. Mass *vs.* age plot for the six stars of the ONC with evidence of Li depletion. For each star, the plot gives the luminosity curve (positive slope) and the Li abundance curve (negative slope) computed for the observed Li abundance. The dashed curves give the uncertainty range in the observed luminosity (±0.2 dex, long-dashed line) and in the measured A(Li) (short-dashed line). The hatched region bounds the values of mass and age consistent with the observations. In each panel, the solid points with error bars give the mass and age from theoretical PMS tracks and isochrones (filled: PS99; open: Siess *et al.* 2000). (From Palla *et al.* 2007.)

fit of the upper main-sequence (*e.g.*, Barrado y Navascués *et al.* 1999; Jeffries & Oliveira 2005; Manzi *et al.* 2008). The general result is that the LDB ages tend to be higher than those estimated from the upper main sequence fitting, although the difference is reduced for the youngest clusters. This difference is attributed to the neglect of convective-core overshoot that allows to mix more hydrogen into the stellar core, thus increasing the main sequence lifetime (by a factor of ∼1.5).

Although the LDB technique is model dependent, the difference in the age obtained using a variety of evolutionary models is modest (±10%; Burke *et al.* 2004) which explains why the method is still largely used. However, because of the intrinsic faintness of the low-mass stars that show the boundary, typically mid- to late-M dwarfs, and the need of high resolution spectra, the number of open clusters with reliable LDB measurements is quite limited. The current census includes six clusters: Pleiades (126 ± 1 Myr; Stauffer *et al.* 1998; Burke *et al.* 2004), α Persei (90 ± 10 Myr; Stauffer *et al.* 1999), IC 2391 (50 ± 5 Myr; Barrado y Navascués *et al.* 1999, 2004), NGC 2547 (35 ± 4 Myr; Jeffries & Oliveira 2005), IC 4665 (27 ± 5 Myr; Manzi *et al.* 2008), Blanco 1 (132 ± 24 Myr; Cargile *et al.* 2010), and IC 2602 (46 ± 6 Myr; Dobbie *et al.* 2010).

The young cluster IC 4665 stands out as the youngest open cluster with an LDB with an age of $\sim 27 \pm 5$ Myr. The model-dependent mass of the boundary

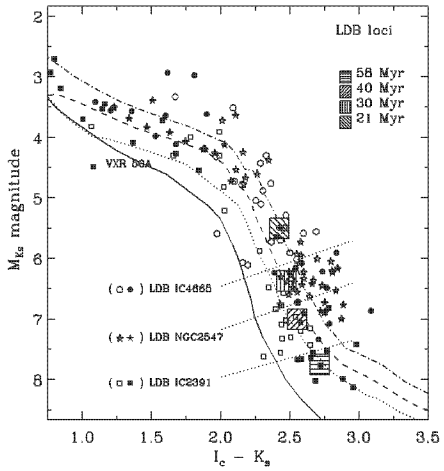

Fig. 10. The distribution of confirmed members of the three youngest open clusters: IC 4665, NGC 2547, and IC 2391 in the K_s *vs.* [I_C–K_s] diagram. Filled and empty symbols represent stars of each cluster with and without lithium, respectively. The hatched squares are the loci of the predicted LDB at different ages according to Baraffe *et al.* (2002). Also shown are several isochrones from the same models, along with the ZAMS (solid line). The light diagonal curves mark the position of the LDB in each cluster, as labeled. (From Manzi *et al.* 2008.)

corresponds to $M_* = 0.24 \pm 0.04\, M_\odot$. Comparison of the LDB age with the standard turn-off age (Mermilliod 1981) and that inferred from isochrone fitting of the cluster low-mass sequence shows an excellent agreement, similar to what found in NGC 2547 (Jeffries & Oliveira 2005). Thus, the difference between the LDB and the isochronal value appears to show itself as a function of age, not unexpectedly if the physical reason for the discrepancy is attributed to convective core overshoot. However, the inconsistency can also reside in the approximations of the PMS models. In particular, the theoretical and empirical bolometric corrections needed to derive the absolute magnitudes in the I_C or K_s band are still affected by systematic uncertainties due to missing physical processes (such as, opacities, magnetic activity, etc.) that are not taken into account in current models. The LDBs for three young clusters are displayed in Figure 10.

7 Revisiting the Orion Nebula Cluster

The ONC is the nearest site of recent massive star formation and serves as a calibrator and prototype for young stellar clusters. It is also the closest system where the entire IMF from $\sim 30\, M_\odot$ down to $10\, M_{Jup}$ can be studied with minimal foreground and background contamination. The cluster has been repeatedly studied with increasing field coverage both in the visible (*e.g.*, Hillenbrand 1997;

Robberto *et al.* 2004) and in the near-IR (*e.g.*, Luhman *et al.* 2000; Slesnick *et al.* 2004; Robberto *et al.* 2010). Thus, it has been possible to identify a population of young, nearly coeval, and uncontaminated of about $1–3 \times 10^4$ stars aged ∼1–3 Myr (Hillenbrand *et al.* 2001).

Until recently, the most complete work on the characterization of the stellar population remained that of Hillenbrand (1997) who performed a spectrophotometric analysis, derived the extinction of ∼1000 members and used the dereddened phothometry to place the stars in the HR diagram. The stellar masses and ages were then derived through comparison with PMS evolutionary models. However, despite the advantages of such an approach, other factors limited the accuracy of the estimate of the fundamental stellar parameters. For example, the nebulosity that surrounds the cluster and the presence of circumstellar material (disks and envelopes) cause highly non-uniform extinction which must be corrected for each star. Also, uncertainties in the conversions between colors and magnitudes to temperatures and luminosities make the construction of an accurate HR diagram based on photometry alone misleading. Even when spectra are available and estimate of the accretion excess can be directly derived, the uncertainty in the spectral type-T_{eff} relation and the difficulty of obtaining spectra in crowded field with bright, variable background emission limits the accuracy in the determination of the stellar parameters.

In order to overcome, or to better assess, the impact of such factors, a new set of ground-based, simultaneous, boradband observations of the ONC has been presented by Da Rio *et al.* (2009), based on observations carried out with the WFI imager at the ESO/MPI 2.2 telescope over a field of about 34×34 arcmin. The sample consists of more than 1000 stars with known spectral type and accurate estimates of the individual extinction and accretion luminosity. Using a more appropriate spectral type–temperature transformation and adopting the revised lower distance to Orion of 414 pc (*e.g.*, Menten *et al.* 2007 from trigonometric parallax), instead of the previously adopted value of 475 pc, Da Rio *et al.* present a new HR diagram, more populated than previous works.

7.1 A new HR diagram

Figure 11 displays the HRD for the ONC using two sets of evolutionary models for masses from 0.1 $M_\odot$ to 3.5 $M_\odot$: Siess *et al.* (2000) and PS99. The sample contains all known members with a contamination from foreground and background sources with unknown membership of only ∼2–3% of the total. The revised lower distance of 414 pc leads to systematically lower luminosities; however, this is compensated by a higher luminosity found for the late-type stars and slightly lower luminosities for early types. The resulting HRDs have been computed using a standard $R = 3.1$ reddening law. As one can see from the figure, a number of sources are located below the ZAMS and under-luminous confirmed members. While the former are likely background objects, the latter can be explained by the presence of an edge-on disk that partially occults the photosphere or scatters a significant fraction of the stellar flux (Kraus & Hillenbrand 2009). Comparison of the two sets of models

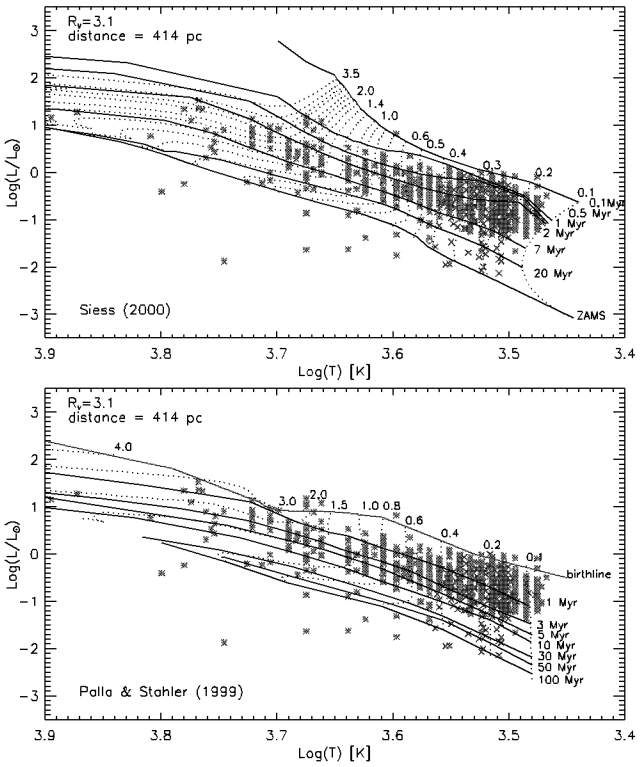

Fig. 11. The HRD for the ONC. Blue stars refer to spectral types from Hillenbrand (1997), excluding sources with membership <50%. Red circles are the newly classified stars from the spectroscopic survey. Green crosses are for the M-type stars whose temperatures are derived from the [TiO] index. (From Da Rio *et al.* 2010.)

shows that both are generally parallel to the median of the observed distribution of stars in the diagram. However, while Siess' models predict that isochrones at a given age are located at higher luminosities (thus implying older ages for the cluster), PS99 results find the opposite. The main conclusion is that *this new version of the ONC HRD still shows the ∼1.5 dex luminosity spread derived from the single epoch observations of Hillenbrand (1997) and its magnitude cannot be attributed solely to observational uncertainties/error and/or intrinsic luminosity variations and/or biases.* This luminosity spread, of course, reflects into an age spread, as we now discuss.

7.2 Age distribution

A fundamental issue when dealing with derived quantities (mass, age) from the distribution of a stellar group from the HR diagram is the completeness of the

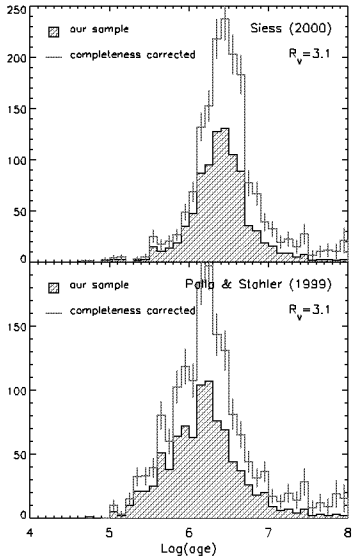

Fig. 12. Age distribution for the ONC sample using the two evolutionary models. The dashed histograms show the age distributions of the sample. The same after correction for completeness are displayed by the thin lines with the statistical uncertainties shown for each age bin. (From Da Rio *et al.* 2010).

sample. This problem is discussed in detail in Da Rio *et al.* (2010), particularly in the context of the mass-age relation introduced by spurious selection effects. For example, if one considers the full sample without careful analysis of the completeness issue, then an apparent increase of the age of the more massive stars is found using the PS99 models. However, this correlation disappears when a careful statistical analysis of the completeness is made.

The age distribution of the complete sample is shown in Figure 12 as derived from the two models. One can see that the completeness correction does not influence significantly the average ages and the measured age spread, but it increases the old age tail of the distributions. In the Siess case, the peak is at ∼3 Myr with a broadening of ∼0.3 dex, while with PS99 the peak is at ∼2 Myr with a higher dispersion of ∼0.4 dex. Within 1σ, the age of the population varies between 2.5 and 5 Myr (Siess) and 1.2–3.2 Myr (PS99).

Whether the age spread observed both in the HRD and in the histogram of Figure 12 is real or not is a basic problem that has already been addressed in the previous Section. It is clear that the age distributions of Figure 12 represent the combined effect of the intrinsic age spread and the apparent one due to other effects that broaden the observed luminosities (mainly, stellar variability and scattered light from circum-stellar material). However, Da Rio *et al.* reach the conclusion that the overall width of the distribution cannot be attributed solely to these

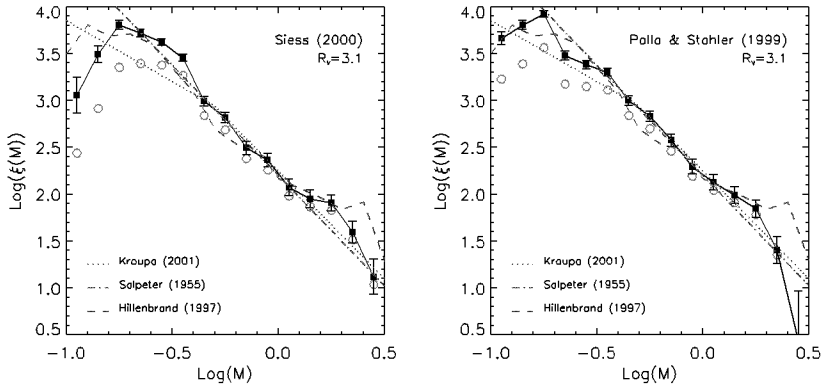

Fig. 13. The two panels show the completeness-corrected (filled circles) and the incomplete (open circles) IMF for the ONC, according to Siess *et al.* (2000) and PS99. Also shown are the empirical IMF of Hillenbrand (1997) and the functional forms of Salpeter (1955) and Kroupa (2001). (From Da Rio *et al.* 2010.)

effects and that a real spread is the main cause of the observed width. This is in agreement with the result found by Jeffries (2007) from a statistical analysis of the geometrically estimated radii.

7.3 Determination of the IMF

Figure 13 shows the IMF for the ONC using the two sets of evolutionary models as before. Also displayed for comparison are other forms of the IMF to highlight differences with the results of Da Rio *et al.* (2010). For example, one can see that Kroupa under-produces the low-mass population and does not reproduce the observed turnover. The general results found by Hillenbrand (1997) are recovered, confirming the flattening at masses below $\sim 0.3\,M_{\odot}$. However, the two sets of models yield significant differences in the low-mass regime: while for PS99 the change of slope from the general power-law is modest and in agreement with Kroupa's (2001) prescription, the Siess models predict a clear turn-over below $0.2\,M_{\odot}$, compensated by an increase in the number of stars between 0.2–$0.3\,M_{\odot}$. Unfortunately, any conclusion about the true shape of the IMF in the very low-mass and BD regime is still hampered by the model-dependent results indicated by this analysis.

An interesting comparison of the IMF of Figure 13 can be made with the results by Muench *et al.* (2002) based on a Monte-Carlo best fit to the observed K-band luminosity function. These authors had found a power-law distribution with slope similar to the Salpeter value, but a flattening at mass $\sim 0.6\,M_{\odot}$, much higher than that obtained by Hillenbrand and Da Rio. The main reason for the difference is that the K-band flux is contaminated by emission due to circumstellar material which biases the estimated toward higher luminosities and hence masses. This is important to keep in mind when deriving IMFs from surveys based only on infrared fluxes.

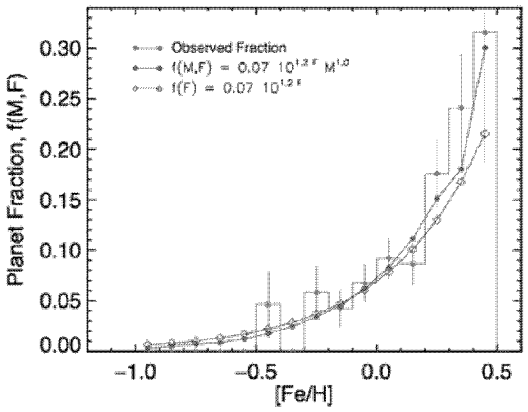

Fig. 14. Planet fraction as a function of metallicity for a sample of 1266 stars drawn from the California Planet Survey. The observed distribution scales as $f \propto 10^{1.2[Fe/H]}$. Also, the planet fraction increases with stellar mass as $f \propto M_*$. (From Johnson *et al.* 2010.)

8 Chemical abundances in star forming regions and young clusters

Along with mass and angular momentum, the chemical composition of a star is a fundamental parameter that determines its evolutionary properties. For example, the metal content, Z, is a critical quantity for the derivation of cluster ages and individual stellar masses. The stellar luminosity is more sensitive to the metallicity than the effective temperature (*e.g.*, Forestini 1994), yielding substantial changes for small variations of Z that affect the evolutionary time scale: the latter increases for larger values of the metallicity. Mayne & Naylor (2008) estimate that a reduction to half a solar composition results in a reduced distance modulus of $\sim$0.5 dex, or a factor of $\sim$2 in age. Therefore, a precise measurement of the metalliicity is required and is vital for accurate determinations of the parameters of SFRs. Until now, the information on the metallicity has been modest and with rather large uncertainties. As we shall see below, the situation has improved in the last few years.

Another important reason for the relevance of abundance determinations is the discovery of the correlation between stellar metallicity and the presence of giant planets (Santos *et al.* 2001). It is now well established that planet-host stars are on average more metal rich than stars without planetary-mass companions (*e.g.*, Johnson *et al.* 2010). The observed correlation between stellar metallicity and planet detection is shown in Figure 14. The mean metallicity of stars hosting a gas giant planet is [Fe/H] = +0.15±0.23, compared to the value [Fe/H] = −0.10±0.18 for the solar neighborhood. What is still unclear is if, besides other factors such as stellar age and mass, the fraction of circumstellar disks (the planet birthplaces) depends on the stellar metallicity. In this context, young clusters with age $\sim$10 Myr are important targets for abundance studies since there is strong indication that by this time the majority of the inner disks have been dissipated and planet formation

is largely completed (Pollack *et al.* 2006). Acquiring information on the metallicity of the stars in this critical age range is hence of obvious relevance.

Finally, the popular model of triggered star formation predicts a peculiar chemical enrichment due to contamination of material ejected from type II SNe originating from a first generation of massive stars (*e.g.*, Reeves 1978). Accordingly, in a given SFR, one would expect a different abundance pattern across the cluster subgroups, with the youngest regions having peculiar chemical enrichment in iron-peak and α-elements. The Orion OB1 association has been long considered as a possible example of triggered star formation (Blaauw 1991) with its four subgroups (Orion Ia-d) characterized by different age, size, and position. In support of this view, Cunha and collaborators (1992, 1998) found evidence of star-to-star variation in oxygen and silicon abundances, with few O- and Si-enhanced stars being more centrally located (in the Trapezium region, Ori Id) than the O- and Si-poor stars, distributed throughout the association. More recent work by Simón-Díaz *et al.* (2006) on a number of B-type stars in the Trapezium derived lower O-abundances than those obtained by Cunha's group and no evidence of any elemental abundance. Considering the importance of the Orion association as the best studied massive star forming complex in the solar vicinity and the general relevance of the triggered mode of star formation for galactic evolution, it is of interest to discuss the recent determinations of chemical abundances in this region and other nearby SFRs.

8.1 Metallicity determination in orion

In addition to the information provided by the massive stars of the Orion complex, low-mass stars in the various subgroups offer an alternative means of studying the metallicity distribution. Initially, Padgett (1996) obtained [Fe/H] values between -0.1 and $+0.23$ dex and an average [Fe/H] slightly above solar for seven stars in Orion Ic and Id. Notably, of the four stars in the ONC, two of them showed higher than solar abundance ([Fe/H] $= 0.14 \pm 0.18$ and 0.08 ± 0.17), while the other two had solar metallicity (-0.01 ± 0.21 and -0.01 ± 0.17, respectively). More recently, based on the analysis of three stars, Santos *et al.* (2008) obtained an average value [Fe/H] $= -0.13 \pm 0.06$ for the ONC, indicating a subsolar metallicity.

Considering the large uncertainty still associated with the various determinations and the conflicting results, a new and homeogenous study of the elemental abundance has been recently completed, including the other young clusters of the Orion associations 25 Ori, λ Ori and σ Ori. The survey was carried out with FLAMES/UVES at ESO that yielded accurate radial velocities and cluster membership for all the targets. The main results are shown in Figure 15 and can be summarized as follows (see D'Orazi *et al.* 2009; Biazzo *et al.* 2011a; Biazzo *et al.* 2011b):

- Iron abundance values are [Fe/H] $= -0.08 \pm 0.15$ for Ori Ia; -0.05 ± 0.05 for Ori Ib; -0.11 ± 0.08 for ONC; -0.02 ± 0.09 for σ Ori; -0.06 ± 0.03 for 25 Ori; and 0.01 ± 0.01 for λ Ori.

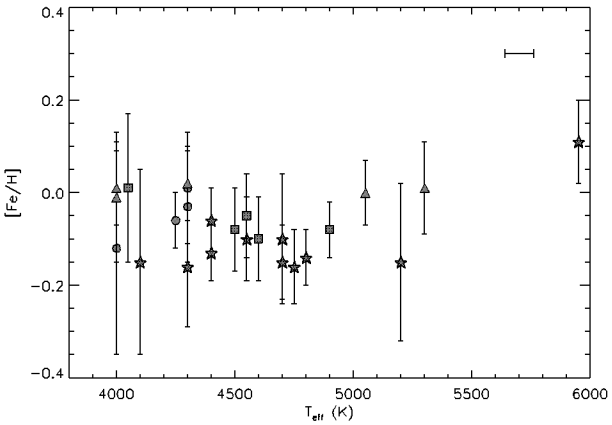

Fig. 15. Iron abundances of low-mass stars in the various clusters of the Orion complex. The star symbols are for the ONC: note the lower abundance relative to the other stars. The point at T_{eff}∼6000 K is for P1455. (From Biazzo *et al.* 2011a, 2011b.)

- With the exception of one star, P1455 in the ONC, which has a metallicity [Fe/H]=0.11±0.09, all the other stars show solar or subsolar abundances, thus confirming indications in other SFRs (see below) on the rarity/paucity of metal-rich stars in the solar neighborhood.
- No star-to-star variation is found for the other heavy elements (Na, Al, Si, Ca, Ti, and Ni), with a high degree of homegeneity within each stellar group.
- The Orion complex is characterized by a small group-to-group dispersion (∼±0.05 dex) in the low-mass stars, consistent with the results found for the massive stars (Simón-Díaz 2010) and the interstellar gas (Simón-Díaz & Stasinska 2010).

Overall, the reconstruction of the metallicity distribution in Orion seems to indicate that each subgroup/cluster followed a different and independent star formation history and that the level of dispersion observed may simply reflect the initially inhomogeneous medium from which the groups originated (*e.g.*, Elmegreen 1998). Also, the fact that the youngest object in Orion, the ONC, has the lowest metallicity, seems to exclude a direct and significant amount of contamination between adjacent regions, as expected in the SN-driven abundance enrichment scenario (*e.g.*, Cunha *et al.* 1998).

8.2 Metallicity in other SFRs and young clusters

How the results obtained for the Orion complex compare to those of other nearby SFRs and older open clusters? This is an interesting question that can be answered thanks to the rather large sample of accurate abundances now available. Considering SFRs first, other than Orion, iron abundances have been obtained in

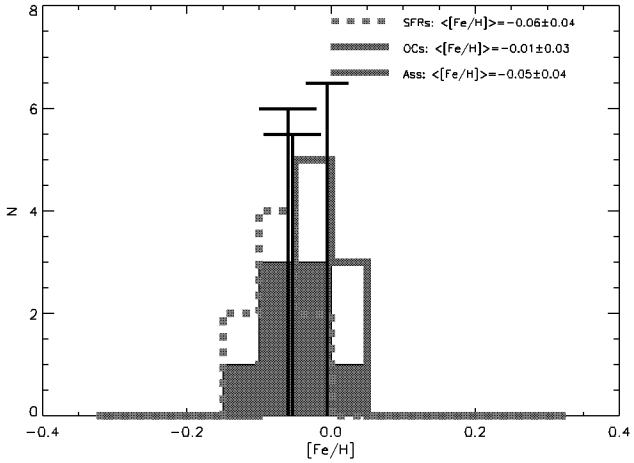

Fig. 16. Distribution of the iron abundance in SFRs (dashed), young open clusters (solid) and associations (shaded). Note the displacement to subsolar values for the SFRs. (Data from Biazzo *et al.* 2011a, 2011b; Santos *et al.* 2008; Viana Almeida *et al.* 2009.)

Chamaeleon, NGC 2264, CrA, Lupus, ρ oph, and Taurus. The average values vary between [Fe/H] $= -0.05 \pm 0.02$ in Lupus (Santos *et al.* 2008) and -0.18 ± 0.08 in NGC 2264 (King *et al.* 2000). Thus, all of the main star forming sites have slightly sub-solar metallicities. This result also holds for the nearby moving groups/stellar associations, as described by Viana Almeida *et al.* (2009) who have analyzed eleven such systems (including AB Dor, β Pic, and ϵ Cha). Solar metallicity is a common result in all of them and the low abundance dispersion within each group supports the idea that their origin is associated with that of the more prominent SFRs.

As to the question of the existence of metal-rich young associations and SFRs, none has been found so far (*cf.* Santos *et al.* 2008). On the other hand, if one considers the distribution of open clusters within 500 pc with an available [Fe/H] determination, one finds that 3/16 (19%) have [Fe/H] > 0.1 dex, while all the rest have the same solar metallicity. Thus, the probability of finding SFRS/young clusters of comparable metallicity is not negligible, at odds with the results obtained so far. However, these iron-rich clusters turn out to be all older than $\sim$200 Myr, with two of them (Hyades and Praesepe) belonging to the Hyades supercluster or stream and thus with a peculiar origin. The majority of the other open clusters are part of the Local Association (or Pleaides moving group) and of the IC 2391 supercluster and they all share the same solar metallicity. The distribution of the iron abundance in SFRs, young clusters and associations of the solar neighborhood is displayed in Figure 16.

8.3 Implications on PMS models and galactic chemical evolution models

In contrast to the statement made at the beginning of this Section on the large effect of metallicity variations on PMS models, the nearly uniform values of

metallicity found in most of the nearby (∼0.5 kpc) SFRs and clusters is good news, implying that one should not worry too much about the effects of this parameter on the individual and global properties of young stars. Although the effect is important in principle, large variations of the metallicity Z are not observed on this scale and one is allowed to reasonably assume standard solar values when interpreting the large amount of data now available on the young stellar populations of SFRs close to the Sun.

As to the comparison of the abundances in SFRs with those observed in field stars, Santos *et al.* (2008) have shown for the volume-limited sample used for planet searches that the two distributions have similar average metallicities (−0.08 for the SFRs and −0.10 for field stars), but significantly different widths: $\sigma = 0.033$ dex and 0.24 dex, respectively. Monte Carlo simulations reinforced the conclusion that the small dispersion of SFRs is at odds with that of field stars and that the former is statistically significant. Since a small dispersion is also found in other components of the solar neighborhood (open clusters, interstellar medium), the implication is that mixing in the ISM is very efficient and in any case it occurs on a time scale shorter than any enrichment event (see, *e.g.*, the discussion in Wielen *et al.* 1996).

Finally, the fact that most SFRs have subsolar metallicity deserves some consideration since it seems to be at odds with the idea supported by galacto-chemical models of a slow chemical enrichment of the galactic disk since the time of the formation of the Sun (*e.g.* Carigi *et al.* 2005). On the other hand, it is possible that either the Sun was formed in a region different than its present location and at small galactocentric distances (*e.g.* Wielen *et al.* 1996) or that the local ISM was diluted as the result of infall of low-metallicity gas.

It is a pleasure to thank the organizers of this School, Corinne Charbonnel and Thierry Montmerle, for allowing me to participate in the program and prepare this contribution (that took longer than anticipated!). I acknowledge very useful conversations with several colleagues and collaborators, including Katia Biazzo, Nicola Da Rio, Willem-Jan de Wit, Bruce Elmegreen, Marcella Marconi, Sofia Randich, Steven Stahler, Keivan Stassun, Hans Zinnecker.

References

Alcalá, J.M., Spezzi, L., Chapman, N., *et al.*, 2008, ApJ, 676, 427

Alecian, E., Catala, C., Van't Veer-Menneret, C., *et al.*, 2005, A&A, 442, 993

Alecian, E., Lebreton, Y., Goupil, M.-J., *et al.*, 2007, A&A, 473, 181

Andersen, J., 1991, A&AR, 3, 91

Asplund, M., Grevesse, N., Sauval, A.J., *et al.*, 2005, A&A, 431, 693

Baglin, A., Auvergne, M., Barge, P., *et al.*, 2007, AIPC, 895, 201

Ballesteros-Paredes, J., Klessen, R.S., Mac Low, M.-M., & Vazquez-Semadeni, E., 2007, in it Protostars and Planets V, 63

Baraffe, I., Chabrier, G., Allard, F., & Hauschildt, P.H., 1998, A&A, 337, 403

Baraffe, I., Chabrier, G., Allard, F., & Hauschildt, P.H., 2002, A&A, 382, 563

Barrado y Navascués, D., Stauffer, J.R., & Patten, B., 1999, ApJ, 522, L53

Barrado y Navascués, D., Bouvier, J., Stauffer, J.R., *et al.*, 2002, A&A, 395, 813

Barrado y Navascués, D, Stauffer, J.R., & Jayawardhana, R., 2004, ApJ, 614, 386
Basri, G., 2000, ARA&A, 38, 485
Basri, G., Marcy, G.W., & Graham, J.R., 1996, ApJ, 458, 600
Bastian, N., Covey, K.R., & Meyer, M.R., 2010, ARA&A, 48, 339
Bernabei, S., Ripepi, V., Ruoppo, A., *et al.*, 2009, A&A, 501, 279
Beuther, H., Churchewell, E.B., McKee, C.F., & Tan, J.C., 2007, in Protostars and Planets V, 165
Bhöm, T., Zima, W., Catala, C., *et al.*, 2009, A&A, 497, 183
Biazzo, K., Randich, S., & Palla, F., 2011, A&A, 525, 35
Biazzo, K., Randich, S., Palla, F., & Briceño, C., 2011, A&A, 530, A19
Bildsten, L., Brown, E.F., Matzner, C.D., & Ushomirski, G., 1997, ApJ, 482, 442
Blaauw, A., 1961, Bull. Astron. Inst. Netherlands, 15, 265
Blaauw, A., 1991, ASI Ser., 342, 155
Bonanos, A.Z., 2009, ApJ, 691, 407
Bonnell, I.A., & Clarke, C.J., 1999, MNRAS, 309, 461
Bonnell, I.A., Bate, M.R., & Zinnecker, H., 1998, MNRAS, 298, 93
Bonnell, I.A., Larson, R.B., & Zinnecker, H., 2007, in Protostars and Planets V, 149
Boudreault, S., Bailer-Jones, C.A., Goldman, B., *et al.*, 2010, A&A, 510, 27
Bouvier, J., Kendall, T., Meeuws, G., *et al.*, 2008, A&A, 481, 661
Burbidge, E.M., Burbidge, G.R., Fowler, W.A., & Hoyle, F., 1957, Rev. Mod. Phys., 29, 547
Burgasser, A.J., Kirkpatrick, J.D., Reid, I.N., *et al.*, 2003, ApJ, 586, 512
Burgess, A.S.M., Moraux, E., Bouvier, J., *et al.*, 2009, A&A, 508, 823
Burke, C.J., Pinnsonneault, M.H., & Sills, A., 2004, ApJ, 604, 272
Cargile, P.A., Stassun, K.G., & Mathieu, R.D., 2008, ApJ, 674, 329
Cargile, P.A., James, D.J., & Jeffries, R.D., 2010, ApJ, 725, L111
Carigi, L., Peimbert, M., Esteban, C., & García-Rojas, J., 2005, ApJ, 623, 213
Chabrier, G., 2003, PASP, 115, 763
Chabrier, G., & Baraffe, I., 2000, ARA&A, 38, 337
Chabrier, G., Gallardo, J., & Baraffe, I., 2007, A&A, 472, L17
Chew, Y.G.M., Stassun, K.G., Prsa, A., & Matheu, R.D., 2009, ApJ, 699, 1196
Corbelli, E., Palla, F., & Zinnecker, H., 2005, The Initial Mass Function 50 Years Later, ASSL, Vol. 327
Covino, E., Frasca, A., Alcalá, J.M., *et al.*, 2004, A&A, 427, 637
Cunha, K., & Lambert, D.L., 1992, ApJ, 399, 586
Cunha, K., Smith, V.V., & Lambert, D.L., 1998, ApJ, 493, 195
D'Antona, F., & Mazzitelli, I., 1997, Mem. Soc. Astron. It., 68, 807
D'Antona, F., Ventura, P., & Mazzitelli, I., 2000, ApJ, 543, L77
Da Rio, N., Robberto, M., Soderblom, D., *et al.*, 2009, ApJS, 183, 261
Da Rio, N., Robberto, M., Soderblom, D., *et al.*, 2010, ApJ, 722, 1092
Degl'Innocenti, S., Prada Moroni, P.G., Marconi, M., & Ruoppo, A., 2008, Ap&SS, 316, 25

De Marchi, G., Paresce, F., & Portegies-Zwart, S., 2005, in The Initial Mass Function 50 Years Later, ASSL, 327, 77

De Marchi, G., Paresce, F., & Portegies-Zwart, S., 2010, ApJ, 718, 105

Demarque, P., Guenther, D.B., & Li, L.H., 2008, Astrophys. Sp. Sci., 316, 31

de Wit, W.J., Testi, L., & Palla, F., *et al.*, 2004, A&A, 425, 937

de Wit, W.J., Testi, L., Palla, F., & Zinnecker, H., 2005, A&A, 437, 247

de Wit, W.J., Bouvier, J., & Palla, F., *et al.*, 2006, A&A, 448, 189

Di Criscienzo, M., Ventura, P., & D'Antona, F., 2008, MNRAS, 389, 325

Dobbie, P.D., Lodieu, N., & Sharp, R.G., 2010, MNRAS, 409, 1002

D'Orazi, V., Randich, S., & Flaccomio, E., *et al.*, 2009, A&A, 501, 973

Dotter, A., Chaboyer, B., & Jevremovic, D., *et al.*, 2008, ApJS, 178, 89

Duquennoy, A., & Mayor, M., 1991, A&A, 248, 485

Elmegreen, B.G., 1998, in Abundance Profiles: Diagnostic tools for galactic history, ASP Conf. Ser. 147, ed. D. Friedli *et al.*, 278

Elmegreen, B.G., 2000, ApJ, 530, 277

Forestini, M., 1994, A&A, 285, 473

García, B., & Mermilliod, J.C., 2001, A&A, 368, 122

Gough, D.O., & Tayler, R.J., 1966, MNRAS, 133, 85

Grevesse, N., & Noels, A., 1993, in Origin and Evolution of the Elements (Cambridge Univ. Press), 14

Grigahcene, A., Dupret, M.-A., Garrido, R., *et al.*, 2006, CoAst, 147, 69

Hartmann, L., Heitsch, F., & Ballesteros-Paredes, J., 2009, Rev. Mex. Astr. Astrofis. Conf. Ser., 35, 66

Hennebelle, P., & Chabrier, G., 2008, ApJ, 684, 395

Hennebelle, P., & Chabrier, G., 2009, ApJ 702, 1428

Hernández, J., Calvet, N., Briceño, C., *et al.*, 2004, AJ, 127, 1682

Hillenbrand, L.A., 1997, AJ, 113, 1733

Hillenbrand, L.A., & White, R.J., 2004, ApJ, 604, 741

Hillenbrand, L.A., Carpenter, J., & Feigelson, E.D., 2001, in From Darkness to Light: Origin and evolution of young stellar clusters, 243, 349

Hoogerwerf, R., de Bruijne, J.H.J., & de Zeeuw, P.T., 2001, A&A, 365, 49

Hosokawa, T., & Omukai, K., 2009, ApJ, 691, 823

Huff, E.M., & Stahler, S.W., 2007, ApJ, 666, 281

Irwin, J., Aigrain, S., Hodgkin, S., *et al.*, 2007, MNRAS, 380, 541

Jeffries, R.D., 2004 in Mixing in Stars, ed. S. Randich *et al.* (ESO Symposia)

Jeffries, R.D., 2007, MNRAS, 381, 1169

Jeffries, R.D., & Naylor, T., 2001, in From Darkness to Light: Origin of Young Stellar Clusters, ed. T. Montmerle & Ph. André (San Francisco: ASP), 633

Jeffries, R.D., & Oliveira, J.M., 2005, MNRAS, 358, 13

Jeffries, R.D., Naylor, T., Devey, C.R., & Totten, E.J., 2004, MNRAS, 351, 1401

Johnson, J.A., Aller, K.M., Howard, A.W., & Crepp, J.R., 2010, PASP, 122, 905

King, J.R., Soderblom, D.R., Fisher, D., & Jones, B.F., 2000, ApJ, 533, 944

Kraus, A.L., & Hillenbrand, L.A., 2007, AJ, 134, 2340

Kraus, A.L., & Hillenbrand, L.A., 2009, ApJ, 704, 531
Kraus, S., Weigelt, G., & Balega, Y.Y., 2009, A&A, 195, 207
Kraus, S., Hofmann, K.H., & Menten, K.M., 2010, Nature, 466, 339
Kritsuk, A.G., Ustyugov, S.D., Norman, M.L., & Padoan, P., 2009, J. Phys. Conf. Ser., 180, 012020
Kroupa, P., 2001, MNRAS, 322, 231
Kroupa, P., Tout, C.A., & Gilmore, G., 1993, MNRAS, 262, 545
Krumholz, M.R., & Tan, J.C., 2007, ApJ, 654, 304
Lada, C.J., & Lada, E.A., 2003, ARA&A, 41, 57
Lebreton, Y., & Michel, E., 2008, Ap&SS, 316, 167
Lehman, H., Vitrichenko, E., & Bychkov, V., *et al.*, 2010, A&A, 514, A34
Lodieu, N., Dobbie, P.D., Deacon, N.R., *et al.*, 2007, MNRAS, 380, 712
Lodieu, N., Zapatero Osorio, M.R., Rebolo, R., *et al.*, 2009, A&A, 505, 1115
Luhman, K.L., 1999, ApJ, 525, 466
Luhman, K.L., 2007, ApJS, 173, 104
Luhman, K.L., Mamajek, E.E., Allen, P.R., & Cruz, K.L., 2009, ApJ, 703, 399
Luhman, K.L., Rieke, G.H., Young, E.T., *et al.*, 2000, ApJ, 540, 1016
Macdonald, J., & Mullan, D.J., 2010, ApJ, 723, 1599
Maíz-Apellániz, J., Walborn, N.R., Halué, H.A., & Wei, L.H., 2004, ApJS, 151, 103
Manzi, S., Randich, S., de Wit, W.J., & Palla, F., 2008, A&A, 479, 14
Marconi, M., & Palla, F., 1998, ApJ, 507, L141
Marconi, M., Ripepi, V., & Palla, F., *et al.*, 2004, Comm. Asteroseism., 114, 61
Marques, J.P., Palla, F., & Goupil, M.-J., 2011, in preparation
Marsh, K.A., Plavchan, P., & Kirkpatrick, J.D., 2010, ApJ, 719, 550
Mason, B.D., Gies, D.R., & Hartkopf, W.I., *et al.*, 1998, AJ, 115, 821
Massey, P., & Hunter, D.A., 1998, ApJ, 493, 180
Mathieu, R.D., Baraffe, I., & Simon, M., *et al.*, 2007, in Protostars and Planets V, 411
Mayne, N.J., & Naylor, T., 2008, MNRAS, 386, 261
McKee, C.F., & Tan, J.C., 2003, ApJ, 585, 850
Menten, K.M., Reid, M.J., Forbrich, J., & Brunthaler, A., 2007, A&A, 474, 515
Mentuch, E., Brandeker, A., & van Kerkwijk, M.H., 2008, ApJ, 689, 1127
Mermilliod, J.C., 1981, A&A, 97, 235
Morales, J.C., Ribas, I., Jordi, C., *et al.*, 2009, ApJ, 691, 1400
Moraux, E., Bouvier, J., & Stauffer J.R., 2007, A&A, 471, 499
Morino, J.-I., Yamashita, T., Hasegawa, T., & Nakano, T., 1998, Nature, 393, 340
Mouschovias, T.C., Tassis, K., & Kunz, M.W., 2006, ApJ, 646, 1043
Muench, A.A., Lada, E.A., Lada, C.J., & Alves, J.F., 2002, ApJ, 573, 366
Mullan, D.J., & Macdonald, J., 2001, ApJ, 559, 353
Nakano, T., Hasegawa, T., Morino, J.-I., & Yamashita., T., 2000, ApJ, 534, 976
O'Dell, C.R., 2001, AJ, 122, 2662
Oey, M.S., King, N.L., & Parker, J.W., 2004, AJ, 127, 1632
Padgett, D.L., 1996, ApJ, 471, 847

Padoan, P., Nordlund, A., Kritsuk, A.G., *et al.*, 2007, ApJ, 661, 972
Palla, F., 2004, Baltic Astr., 13, 349
Palla, F., & Stahler, S.W., 1993, ApJ, 418, 414
Palla, F., & Stahler, S.W., 1999, ApJ, 525, 772 (PS99)
Palla, F., & Stahler, S.W., 2000, ApJ, 540, 255
Palla, F., & Stahler, S.W., 2001, ApJ, 553, 299
Palla, F., & Stahler, S.W., 2002, ApJ, 581, 1194
Palla, F., Randich, S., Flaccomio, E., & Pallavicini, R., 2005, ApJ, 626, L49
Palla, F., Randich, S., Pavlenko, Ya.V., Flaccomio, E., & Pallavicini, R., 2007, ApJ, 659, L41
Parker, R.J., & Goodwin, S.P., 2007, MNRAS, 373, 295
Pflamm-Altenburg, J., & Kroupa, P., 2006, MNRAS, 404, 1564
Pflamm-Altenburg, J., & Kroupa, P., 2007, MNRAS, 375, 855
Pflamm-Altenburg, J., & Kroupa, P., 2010, MNRAS, 404, 1564
Pollack, J.B., Hubickyj, O., Bodenheimer, P., *et al.*, 2006, Icarus, 124, 62
Reach, W.T., Faied, D., Rho, J., *et al.*, 2009, ApJ, 690, 683
Reeves, H., 1978, A&A, 19, 215
Ripepi, V., Marconi, M., & Bernabei, S., *et al.*, 2003, A&A, 408, 1047
Ripepi, V., Marconi, M., & Palla, F., *et al.*, 2006, Mem. Soc. Astron. It., 77, 317
Robberto, M., Song, J., & Mora Carrillo, G., *et al.*, 2004, ApJ, 606, 952
Robberto, M., Soderblom, D., Scandariato, G., *et al.*, 2010, ApJ, 139, 950
Ruoppo, V., Marconi, M., Marques, J.P., *et al.*, 2007, A&A, 466, 261
Sacco, G.G., Randich, S., Franciosini, E., *et al.*, 2007, A&A., 462, L23
Salpeter, E.E., 1955, ApJ, 121, 161
Salpeter, E.E., 2002, ARA&A, 40, 1
Santos, N.C., Israelian, G., & Mayor, M., 2001, A&A, 480, 889
Santos, N.C., Melo, C., James, D.J., *et al.*, 2008, A&A, 480, 889
Schatzman, E., 1996, ARA&A, 34, 1
Schertl, D., Balega, Y.Y., Preibisch, Th., & Weigelt, G., 2003, A&A, 402, 267
Scholz, A. Geers, V., Jayawardhana, R., *et al.*, 2009, ApJ, 702, 805
Sestito, P., Palla, F., & Randich, S., 2008, A&A, 487, 965
Siess, L., Dufour, E., & Forestini, M., 2000, A&A, 358, 593
Simón-Díaz, S., 2010, A&A, 510, 22
Simón-Díaz, S., & Stasinska G., 2010, A&A, 562, 48
Simón-Díaz, S., Herrero, A, Esteban, C., & Najarro, F., 2006, A&A, 448, 351
Slesnick, C.L., Hillenbrand, L.A., & Carpenter, J.M., 2004, ApJ, 610, 1045
Smith, R.J., Longmore, S., & Bonnell, I., 2009, MNRAS, 400, 1775
Song, I., Bessell, M.S., & Zuckerman, B., 2002, ApJ, 581, L43
Stahler, S.W., & Palla, F., 2004, The Formation of Stars (Wiley-VCH)
Stahler, S.W., Palla, F., & Ho, P.T.P., 2000, in Protostars and Planets IV, 327
Stassun, K.G., Mathieu, R.D., Vaz, L.P.R., *et al.*, 2004, ApJS, 151, 357
Stassun, K.G., Mathieu, R.D., & Valenti, J.A., 2006, Nature, 440, 311

Stassun, K.G., Mathieu, R.D., Cargile, P.A., *et al.*, 2008, Nature, 453, 1079
Stassun, K.G., Henn, L., López-Morales, M., & Prsa, A., 2009, in The Ages of Stars, IAU Symp., 258, 161
Stauffer, J.R., Schultz, G., & Kirkpatrick, J.D., 1998, ApJ, 499, L199
Stauffer, J.R., *et al.*, 1999, ApJ, 527, 219
Stempels, H.C., Hebb, L., Stassun, K.G., *et al.*, 2008, A&A, 481, 747
Suran, M., Goupil, M., Baglin, A., *et al.*, 2001, A&A, 372, 233
Tan, J.C., Krumholz, M.R., & McKee, C.F., 2006, ApJ, 641, L121
Testi, L., Palla, F., & Natta, A., 1999, A&A, 342, 515
Testi, L., Tan, J.C., & Palla, F., 2010, A&A, 522, 44
Tognelli, E., Prada Moroni, P.G., & Degl'Innocenti, S., 2011, A&A, in press [arXiv:1107.2318]
Torres, C.A.O., Quast, G.R., da Silva, L., *et al.*, 2006, A&A, 460, 695
Viana Almeida, P., Santos, N.C., Melo, C., *et al.*, 2009, A&A, 501, 965
Vitrichenko, E.A., Klochkova, V.G., & Tsymbal, V.V., 2006, Astrophysics, 49, 96
Weidner, C., Kroupa, P., & Bonnell, I.A., 2010, MNRAS, 401, 275
Weigelt, G., Balega, Y.Y., Preibisch, Th., *et al.*, 1999, A&A, 347, L15
White, R.J., & Hillenbrand, L.A., 2005, ApJ, 621, L65
Wielen, R., Fuchs, B., & Dettbarn, C., 1996, A&A, 314, 438
Yee, J.C., & Jensen, E.L.N., 2010, ApJ, 701, 303
Zinnecker, H., & Yorke, H.W., 2007, ARA&A, 45, 481
Zuckerman, B., Song, I., Bessell, M.S., & Webb, R.A., 2001, ApJ, 562, L87
Zwintz, K., 2008, ApJ, 673, 1088
Zwintz, K., Hareter, M., Kuschnig, R., *et al.*, 2009, A&A, 502, 239